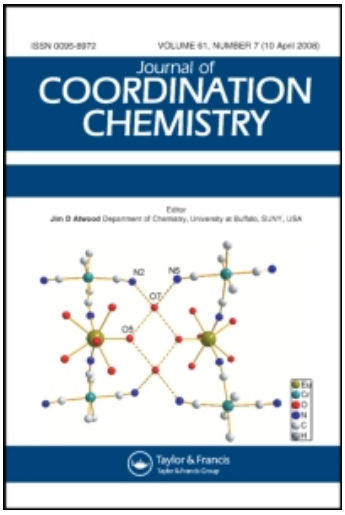

Journal of Coordination Chemistry
Publication details, including instructions for authors and subscription information:
http://www.informaworld.com/smpp/title~content=t713455674

Mechanistic studies of reactions of coordination compounds. Some recent highlights

Colin D. Hubbard[a]; Rudi van Eldik[a]
[a] Institute for Inorganic Chemistry, 91058 Erlangen, Germany

To cite this Article Hubbard, Colin D. and van Eldik, Rudi(2007) 'Mechanistic studies of reactions of coordination compounds. Some recent highlights', Journal of Coordination Chemistry, 60: 1, 1 — 51
To link to this Article: DOI: 10.1080/00958970601089200
URL: http://dx.doi.org/10.1080/00958970601089200

Journal of Coordination Chemistry
Vol. 60, No. 1, 10 January 2007, 1–51

Taylor & Francis
Taylor & Francis Group

Review article

Mechanistic studies of reactions of coordination compounds. Some recent highlights

COLIN D. HUBBARD and RUDI VAN ELDIK*

Institute for Inorganic Chemistry, University of Erlangen-Nürnberg,
Egerlandstrasse 1, 91058 Erlangen, Germany

(*Received 26 September 2006; revised 28 October 2006; in final form 29 October 2006*)

Detailed kinetics studies of reactions of coordination compounds in solution have been invaluable in determining the relevant reaction mechanisms. A selection of reports that highlights very recent progress in mechanistic investigations of coordination chemistry is presented. The methods and techniques employed in pursuit of these mechanistic goals are referred to mostly through the latest authoritative reports. Reactions chosen for inclusion are classified according to the comprehensive table of contents. In summary, solvent exchange, ligand substitution, redox reactions, some reactions of nitric oxide and a few other reactions, whose mechanisms have been scrutinised, are covered.

Keywords: Coordination chemistry reactions; Kinetics; Mechanisms; Activation parameters; Volume profiles

Contents

Abbreviations 2
1. Introduction 4
1.1. *History, and scope of the review* 4
1.2. *Experimental considerations* 5
1.3. *Background theory* 6
1.4. *Reaction selection* 7
2. Recent highlights of mechanistic studies in coordination chemistry 7
2.1. *Solvent exchange* 7
2.1.1. Water exchange at iron(III) 8
2.1.2. Solvent exchange on lanthanide complexes 10
2.1.3. Kinetics of water exchange on hexa-aqua copper(II) and copper(II) complexes 11
2.2. *Ligand substitution reactions* 14
2.2.1. Solvent tuning of the kinetics of ligand substitution of a seven-coordinate iron(III) complex 14
2.2.2. Formation of terpyridine complexes from aqua-ions of Co(II), Ni(II), Cu(II) and Zn(II) 15

*Corresponding author. Email: vaneldik@chemie.uni-erlangen.de

Journal of Coordination Chemistry
ISSN 0095-8972 print/ISSN 1029-0389 online © 2007 Taylor & Francis
DOI: 10.1080/00958970601089200

2.2.3. Ligand substitution at aqua-ruthenium(III)(edta) 17
2.2.4. Substitution at square planar platinum(II) 18
2.2.4.1. Nucleophilic substitution at $[Pt^{II}(N\text{-}N)(H_2O)_2]^{2+}$ complexes 18
2.2.4.2. Substitution reactions of ternary Pt(II) complexes with biologically relevant ligands 20
2.2.4.3. Solvent effects on nucleophilic substitution reactions of $[Pt^{II}(L^3)Cl]^+$ complexes 21
2.2.4.4. Substitution reactions of $[Pt(bmpa)(H_2O)]^{2+}$ and $[Pd(bmpa)(H_2O)]^{2+}$ 22
2.2.5. Kinetics of lanthanum(III) complexation of acetohydroxamic acid 23
2.3. *Redox reactions* 24
2.3.1. Electron transfer reaction between phenothiazines and hexa-aquairon(III) 24
2.3.2. Oxidation of cytochrome c by tris(oxalato)cobalt(III) 26
2.3.3. The outer-sphere electron transfer between cytochrome c and an anionic Cu(II/I) complex 27
2.4. *Reactions of NO in coordination chemistry* 30
2.4.1. Mechanistic studies on the reversible binding of nitric oxide to metmyoglobin 31
2.4.2. The mechanism of nitrite ion binding to metmyoglobin and methaemoglobin 32
2.4.3. Kinetic and mechanistic studies on the reaction of water-soluble iron(III) porphyrin complexes 34
2.5. *Other reactions* 39
2.5.1. Transition state characterisation for reversible binding of dihydrogen to $(bpy)_2$rhodium(I) 39
2.5.2. The kinetics of dissociation of tris(diimine)iron(II) complexes 40
2.5.3. Dynamics of fluxional motion in platinum phenanthroline complexes containing phosphorus donor atoms 42
2.6. *Computational aspects* 43
2.6.1. Nitric oxide binding to cobalamin: influence of the metal oxidation state 43
2.6.2. Ligand exchange processes on solvated beryllium cations 44
2.6.3. Ligand exchange processes on solvated lithium cations 45
3. Concluding comments 46
Acknowledgements 47
References 47

Abbreviations

The abbreviations are those used in the literature cited

aaa	Diethylenetriamine
am	Amino acid
apa	2,6-*bis*-Aminomethylpyridine

bmpa	*bis*(2-Pyridylmethyl)amine
bpy	2,2′-Bipyridine
$cdta^{4-}$	*trans*-1,2-Diaminocyclohexanetetraacetic acid
Cisplatin	*cis*-$[Pt(NH_3)_2Cl_2]$
Cob(II)alamin	Model system for reduced cobalamin
Cob(III)alamin	Model system for cobalamin
Cyclen	1,4,7,10-Tetracyclododecane
Cyt c	Cytochrome c
DFT	Density functional theory
Dien	Diethylenetriamine
DMF	Dimethylformamide
Dmphen	2,9-Dimethyl-1,10-phenanthroline
DMSO	Dimethylsulphoxide
Dmtu	Dimethylthiourea
α,β-$Eddadp^{4-}$	α,β-Ethylenediaminediacetatediproprionate
$Edds^{4-}$	*s,s*-Ethylenediaminedisuccinate
$Edta^{4-}$	Ethylenediaminetetraacetate
Fer(ferene)	(3-(2-Pyridyl)-5,6-*bis*(5-furylsulphonic acid)-1,2,4-triazine
Fertri(ferenetriazine)	(3-(2-Pyridyl)-5,6-*bis*(2-furyl)-1,2,4-triazine
Fz(ferrozine)	5,6-*bis*(4-Sulphonatophenyl)-3-(2-pyridyl)-1,2,4-triazine
5′-GMP	Guanosine-5′-monophosphate
GSH	Glutathione
H_2dapsox	2,6-Diacetylpyridine-*bis*(semioxamazide)
5′-IMP	Inosine-5′-monophosphate
INO	Inosine
L-Met	L-Methionine
MES	4-Morpholineethanesulphonic acid
MetHb	Methaemoglobin
MetMb	Metmyoglobin
Me_3tren	2,2′,2″-tri(N-monomethylamino)triethylamine
Me_6tren	2,2′,2″-tri(N,N-dimethylamino)triethylamine
N7-guo	Guanosine
Pap	*bis*(2-Pyridylmethyl)amine
$(P)Fe^{III}$	Iron(III) porphyrin
$(P^{8-})Fe^{III}$	$5^4,10^4,15^4,20^4$-tetra-*tert*-butyl-$5^2,5^6,15^2,15^6$-tetrakis[2,2-*bis*(carboxylato)ethyl]-5,10,15,20-tetraphenylporphyrin
$(P^{8+})Fe^{III}$	[5,10,15,20-tetrakis-4′-*tert*-butylphenyl-2′,6′-*bis*-(N-methylene-(4″-*tert*-butylpyridinium))porphyrinato]-iron(III) octabromide
$1,3\text{-}Pdta^{4-}$	1,3-Propylenediaminetetraacetate
$Phdta^{4-}$	*trans*-1,2-Diaminephenyltetraacetate
Phen	1,10-Phenanthroline
ppp	Terpyridine
Promazine	Dimethyl-(3-phenothiazin-10-yl-propyl)-amine
Promethazine	Dimethyl-(2-phenothiazin-10-yl-propyl)-amine
Pt(amp)	$[Pt(aminomethylpyridine)(H_2O)_2]^{2+}$
Pt(bpy)	$[Pt(N,N\text{-}bipyridine)(H_2O)_2]^{2+}$
Pt(dach)	$[Pt(diaminocyclohexane)(H_2O)_2]^{2+}$
Pt(en)	$[Pt(ethylenediamine)(H_2O)_2]^{2+}$

$[R^1C(=O)N(OH)R^2]$	Hydroxamic acid: $R^1 = CH_3$, $R^2 = H$, HA = acetohydroxamic acid
S-Cyst	L-Cysteine
Terpy	2,2′:6′,2″-Terpyridine
Tmpa	*tris*(2-Pyridylmethyl)amine
Tmtu	Tetramethylthiourea
Tmu	N,N,N′,N′-Tetramethylurea
Tren	2,2′,2″-Triaminotriethylamine
Tu	Thiourea

1. Introduction

1.1. *History, and scope of the review*

The most common approach for determining reaction mechanisms of chemical reactions of coordination complex species is the interpretation of results from kinetics investigations. Early studies sought mechanistic linkage, or comparison with established organic chemistry mechanisms [1–3]. Important literature from relatively few laboratories engaged in mechanistic endeavours stimulated a more widespread recognition of a new sub-discipline within inorganic chemistry [4–8]. Previously the emphasis was mostly on preparative, descriptive, structural, bonding, stereochemical and spectroscopic (methods developed at the time) aspects. Although the subject of coordination chemistry was treated in standard inorganic chemistry textbooks of the time [9–11], kinetics and mechanistic considerations of solution reactions of coordination complexes were not yet included for consumption by students. For obvious reasons, at the time, only relatively inert reactions were accessible for a kinetics examination. However, many reactions of transition metal-based coordination compounds in solution are rapid and their kinetics could only be studied upon the advent of specialised or fast reaction instrumentation [12–14], although some forms of rapid reaction methods had been employed in biochemistry applications for some time [15–19]. Initially, fast reaction studies were confined to research groups where the apparatus was fabricated locally. Progress in fast reaction capability as applied to all types of reaction was reported extensively. A rapid-mixing method, the stopped-flow (sf) method, named because of a method of stopping the flow rapidly before reaction monitoring begins, has endured as a far more versatile method of measurement for coordination chemistry reaction kinetics, than relaxation methods. The time resolutions of the latter are superior (much faster reactions can be studied), but the properties of the reaction system required for the system to be amenable to relaxation methods are more restrictive. Examples of the earliest reactions of coordination chemistry employing rapid reactions methods may be examined in the literature of almost 50 years ago [20–23]. Commercial availability of the sf method heralded a massive growth in studies of rapid reactions of coordination compounds. There was a renewed interest in conventional time range reactions. Chronicling these and subsequent findings on kinetics studies of coordination compounds in addition to the original literature were a range of specialised texts or review series or individual reviews, a selection of which is referenced [24–32].

Several possible variables may be employed in a comprehensive kinetics study. Measurement of the kinetic properties as a function of hydrostatic pressure may be thought of as the most valuable addition to the kineticist's repertoire in inorganic chemistry, in coordination chemistry in particular [33, 34], and to an extent in organometallic chemistry [35], in the past four decades. Relatively few research groups possess the capability to conduct kinetics investigations at elevated pressures. Nevertheless, an examination of literature compilations of results from these investigations provides an illustration of the volume of research conducted; for example, in the period 1987–1996, about 1500 entries of kinetic parameters from principally coordination chemistry and including a few from bioinorganic chemistry and organometallic chemistry were reported [36].

This review will consist of a selection of highlights of kinetics and mechanistic studies of coordination chemistry reactions from mostly, recent reports. An exhaustive survey over a recent period of all the literature would not be realistic. Therefore the choice is somewhat subjective, but does not imply that reports that are not included are not significant. Several quite recent review articles have covered various aspects of the relevant kinetics literature [37–39]. These include chapters in books, a Chemical Review issue dedicated to Inorganic and Bioinorganic Mechanisms [32], individual articles within and a whole issue dedicated to pertinent kinetics studies in Advances in Inorganic Chemistry [40]. These provide a broad background and a reasonably contemporary assessment of the subject up to a few years ago.

1.2. *Experimental considerations*

The experimental aspects of kinetics measurements, for example the determination of rate laws, and their interpretation, and the use of the Eyring equation to derive the enthalpy and entropy of activation have been described thoroughly in standard literature and will not be repeated here [41]. Details of the instrumentation used in kinetics measurements have been presented on several occasions, and since only slight incremental developments have occurred since the appearance of these publications, the principal information regarding apparatus, techniques and methods may be obtained from these sources [42–59]. In this article reaction initiation will be limited almost entirely to standard thermal methods, and reactions initiated photolytically, electrochemically or following pulse radiolysis have recently been authoritatively described [60–62] and will not be included here. The principal method of monitoring reactions of coordination compounds is by UV/visible spectrophotometry as many reactions of transition metal complexes are accompanied by changes in the electronic spectra. In cases when the reaction involves no net change, such as in solvent exchange processes, appropriate choice of a magnetically sensitive nucleus may allow the reaction to be followed directly or as result of enrichment of a particular isotopic form of the solvent by nuclear magnetic resonance (NMR) spectroscopy. As noted above, a wide range of reaction half-lives may be encountered. The publications cited earlier address measurement techniques for both fast and conventional time range reactions, and also describe the adaptation of instruments for monitoring reactions at elevated pressures for both conventional time range instruments, and for high pressure sf (hpsf) and high pressure NMR (hpNMR) spectroscopy.

1.3. *Background theory*

Since derived parameters from kinetic measurements at elevated pressures have been shown to be very valuable in many cases in diagnosing reaction mechanisms, it is worthwhile to present here a brief re-familiarisation of the basic facts. Standard thermodynamics and transition state theory yield equations (1) and (2).

$$\Delta V = \left(\frac{\delta \Delta G}{\delta P}\right)_{\mathrm{T}} = \left(\frac{-\delta \ln K_{\mathrm{P}}}{\delta P}\right)_{\mathrm{T}} \cdot RT \tag{1}$$

$$\Delta V^{\neq} = \left(\frac{\delta \Delta G^{\neq}}{\delta P}\right)_{\mathrm{T}} = \left(\frac{-\delta \ln k_{\mathrm{P}}}{\delta P}\right)_{\mathrm{T}} \cdot RT. \tag{2}$$

ΔV and $\Delta V^{\neq}$ are the terms that may be derived from measurement of the equilibrium constant, K, for an equilibrium system, and the rate constant, k, for a reaction as a function of pressure, respectively. ΔV is the reaction volume, the difference between the partial molar volume(s) of the product(s) and the reactant(s), while $\Delta V^{\neq}$ is the volume of activation, the difference between the partial molar volume of the transition state and the reactant(s) state. ΔG and $\Delta G^{\neq}$ correspond to the Gibbs free energy for the overall reaction and the Gibbs free energy of activation, respectively, T is the absolute temperature, P is the hydrostatic pressure and R is the ideal gas constant. Clearly the reaction volume can be obtained if K can be determined at various pressures. The form of equation (2) usually used for determining $\Delta V^{\neq}$ is:

$$\ln k_{\mathrm{P}} = \ln k_0 - \left(\frac{\Delta V^{\neq}}{RT}\right) \cdot P. \tag{3}$$

In equation (3), k_{P} is the rate constant at different pressures and k_0 is the rate constant at zero pressure. The latter is practically the same as the value of k at ambient pressure. A plot of $\ln k_{\mathrm{P}}$ *versus* P leads readily to the volume of activation if the plot is linear. Providing the pressure range used, typically 0 to 150 MPa, is not exceeded non-linearity of the plot is rarely observed, particularly when water is the solvent. Non-kinetic effects of pressure upon properties of solvents and management of non-linear plots have been addressed in several sources [46, 63–65]. These potential complications have not been encountered in the reports cited in this review. The reaction volume may be obtained independently if the volume of activation can be obtained for both forward and reverse reactions. As with the activation parameters derived from temperature dependence studies, the volume of activation can be interpreted with less equivocation if it refers to an individual kinetic process. Nevertheless even in that ideal situation, interpretation can be clouded by the need to apportion the measured value of $\Delta V^{\neq}$ to intrinsic and solvation contributions equation (4).

$$\Delta V^{\neq} = \Delta V^{\neq}_{\mathrm{int}} + \Delta V^{\neq}_{\mathrm{solv}} \tag{4}$$

The former refers to mechanistic features such as complete or partial bond breakage or bond formation that contribute to the volume change upon attainment of the transition state. Compilations of volumes of activation for many reactions can be examined to assess typical numerical values for these features; [36, 66, 67], examples of reactions in later sections will also provide illustrative values of these contributions. Suffice to note here that for reactions of coordination compounds, values of $\Delta V^{\neq}$

usually fall within the range from -30 to $+30\,cm^3\,mol^{-1}$. In the extremities of this range, rate acceleration or rate retardation is a factor of about three and a half for a pressure of 100 MPa relative to ambient pressure. Most reactions encountered do not yield values of $\Delta V^{\neq}$ approaching the extremes of this guideline range as can be seen in the extensive tabulations in [36, 66, 67]. Solvation contributions occur when there is a change in charge or polarity in proceeding from the reactant state to the transition state. Surrounding solvent is restricted in volume upon a charge increase, and the converse situation applies. The term electrostriction is commonly used for solvent volume reduction arising from charge increase. Clearly the magnitude of this contribution will depend on the magnitude of charge or polarity change, and will vary with solvent. However, as with the reaction and activation enthalpies (ΔH, $\Delta H^{\neq}$) and entropies (ΔS, $\Delta S^{\neq}$), interpretation of ΔV and $\Delta V^{\neq}$, except in cases of series of very similar reactions, depends upon evaluating the particular conditions and details of each reaction. The volume of activation is not particularly sensitive to temperature, and therefore comparison or contrast between values determined at different temperatures for different reactions may be made. For a given reaction the difference in values of the volume of activation at temperatures 20°C apart would normally be smaller than the experimental error on each value.

1.4. *Reaction selection*

The reactions that form section 2 will be divided into reaction classifications normally used in this context. First solvent exchange processes will be covered, followed by ligand substitution reactions; these will not be subdivided further depending on the coordination number of the central metal atom, but only as individual topics or a group of related reports. A section on redox reactions will continue the selection and this will be followed by a section devoted to reactions of nitric oxide with coordination compounds. This last section will of course include some ligand substitution and redox reactions. However, it seemed convenient to collect together reactions of NO in one section in an attempt at coherence rather than scatter them throughout the narrative. Two final sections will cover reactions not readily amenable to earlier classifications, and a section on theoretical calculations relating to reactions of coordination complex species. Clearly when theoretical work has been carried out in concert with an experimental study it could be noted in more than one section. The contents are quite detailed, enabling readers to be directed to topics of special interest to them.

2. Recent highlights of mechanistic studies in coordination chemistry

2.1. *Solvent exchange*

Although there is no net reaction involved, the understanding of solvent exchange processes can be very important with respect to understanding the lability of metal complexes and the mechanism followed in complex-formation reactions. The kinetics of water exchange on some aqua transition metal ions in oxidation state two were described in the earliest reports in this area almost five decades ago [12]. Since then, there has been a veritable abundance of kinetics studies on solvent exchange on many

fully solvated transition metal ions and on some main group solvated cations. Similar studies have illustrated the mechanism for water exchange on monohydroxy-aquated transition metal ion species, or solvent exchange on fully solvated lanthanide ions and in some cases on partly solvated lanthanide ions, and in a few cases on metal ions of the actinide series. When theoretical calculations on solvent exchange mechanisms have been made, in most cases there is agreement with experimental findings and interpretations. For a while controversy arose when it was claimed, on the basis of calculations, that all first row transition metal aqua-ions of oxidation state two exchanged water molecules by an interchange-dissociative (I_d) mechanism, a conclusion that varied with interpretation of experimental results. Later calculations seemed to resolve the controversy and a mechanistic changeover from an interchange-associative (I_a) mechanism to an I_d mechanism occurs in proceeding from $Mn(aq)^{2+}$ to $Fe(aq)^{2+}$. It is pertinent to note that values of volumes of activation for water exchange were significant factors in the mechanistic distinction. The vast preponderance of results has emanated from the Merbach-Lausanne group, and several comprehensive reviews have appeared [68–70]. These reviews should be consulted for the extensive tabulations of kinetics parameters relating to the exchange processes described so far. Because the subject has been reviewed expertly, thoroughly and recently, in this account we have selected only three aspects of solvent exchange for inclusion. The first will illustrate how the nature of chelating ligands affects the rate of water exchange for the remaining water molecule for a given metal centre (Fe(III)). This leads to a second topic that covers the search for complex ions of lanthanides, especially those of Gd(III), that have appropriate properties of water exchange that render them suitable as agents for magnetic resonance imaging (MRI) in medicinal chemistry applications. A third area of interest is one in which coordinating ligands not only influence the rate of water exchange, but the influence arises principally because the coordinating ligands modify the coordination geometry from that present in the fully aquated metal ion; specifically the metal in question is Cu(II).

2.1.1. Water exchange at iron(III). Polyaminocarboxylate ligands such as edta have been employed widely in coordination and analytical chemistry. When ligands of this type are chelated to a Fe(III) centre it has been pointed out that the coordination number of iron can change from six to seven [71, 72]. A study of the consequences of using different chelating ligands (L) in $[Fe^{III}(L)(H_2O)_x]^{n-}$ upon the rate and mechanism of water exchange was undertaken [73]. The purpose was to answer the following question. How, upon varying systematically the potentially hexadentate ligands with respect to the bridging groups of the diamine function, the chelate ring size, lengthening the carboxylate arms or introducing substituents upon them, could a coherent pattern of lability and mechanism emerge? The ligands used are illustrated with their abbreviations and full names in scheme 1. NMR spectroscopy using ^{17}O in H_2O^{17} at ambient and elevated pressures over a range of temperatures was used to characterise the kinetics properties of water exchange in these Fe(III) complexes and derive from them activation parameters. The kinetics of water exchange on $Fe(H_2O)_6^{3+}$ and $Fe(H_2O)_5(OH)^{2+}$ have been investigated some time ago [74, 75]. The rate constant for exchange at 298 K, $\Delta H^{\neq}$, $\Delta S^{\neq}$ and $\Delta V^{\neq}$ were respectively for the hexa-aqua and the monohydroxo species 1.6×10^2 and $1.4 \times 10^5\,s^{-1}$, 64 and 42 kJ mol^{-1}, -5.4 and $+7.0\,J\,mol^{-1}\,K^{-1}$, and -5.4 and $+7.0\,cm^3\,mol^{-1}$, respectively. The former volume of

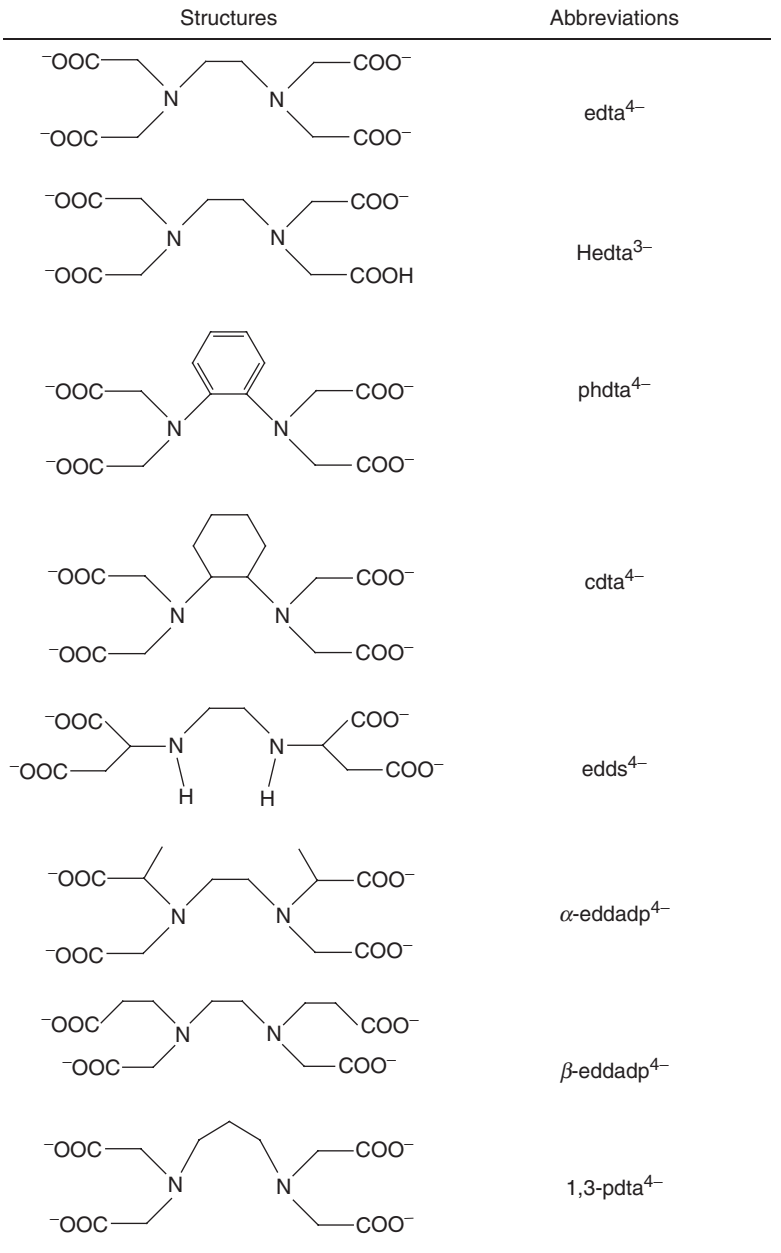

Scheme 1. Multidentate ligands.

activation value was interpreted as indicative of an I_a mechanism, whereas the latter positive value pointed to an I_d mechanism. The marked acceleration (a factor of 10^3) observed upon deprotonating the hexa-aqua Fe(III) species was ascribed to the *trans* effect of coordinated hydroxide on the departing ligand, and this also is the effect suggested to account for the change in mechanism.

The coordination number of the Fe(III) complexes of the ligands in scheme 1 has been established from X-ray crystal structure data. Complexes of edta and phdta exhibit exclusively seven-coordinate geometry, whereas complexes of other ligands, for example those of 1,3-pdta^{4-} and α-eddadp^{4-}, display octahedral geometry in the solid state, that is without a coordinated water. However, the coordination geometry of the latter two complexes in solution remains uncertain. In the edta complex the five-membered chelate rings together with the volume of the central metal ion combine to disfavour octahedral geometry. An earlier study had found that the phdta ligand induced a five orders of magnitude labilisation of the water exchange rate, and high pressure kinetics measurements had led to a volume of activation of $+4.6\,cm^3\,mol^{-1}$ [76]. An I_d mechanism for water exchange was assigned based on that value. Most values of the rate constants for water exchange were measured at or close to a pH of 4. Measurements of water exchange rates on the monoprotonated (Hedta) complexes of Fe(III) were carried out at pH 1. Without exception, and in concert with the available result for the phdta complex, the presence of the chelating ligand enhances the water exchange rate by orders of magnitude, in some cases six orders over the rate of water exchange on the hexa-aqua Fe(III) species. The least acceleration occurred in the complex of edds, and indeed the value of $\Delta V^{\neq}$ of $-14.4\,cm^3\,mol^{-1}$ suggested the operation of a limiting associative mechanism in this case. Scrutiny of the results indicated that the nature of the diamine backbone had little effect on the water exchange rate, and a similar finding prevailed for the effect of methyl substitution on the carboxylate arm. Except as cited for the edds complex, the volumes of activation were all modestly positive, and the common property of rate acceleration was attributed to the labilising influence of the polyamine carboxylate ligands and the change in coordination number from six to seven. The small volumes of activation, typically in the range +2 to $+5\,cm^3\,mol^{-1}$ would ordinarily be characteristic of an I_d mechanism. However, since a significant ground state labilisation could give rise to lengthening of the ground state Fe–OH_2 bond, this modest volume change may mask much larger values of the volume of activation that could result from a tendency toward a limiting D-mechanism.

2.1.2. Solvent exchange on lanthanide complexes. A considerable volume of experimental work, supported in many cases by theoretical studies has been reported on the coordination number and kinetic properties related to solvent exchange on several of the lanthanide ions mostly in oxidation number three [68, 69]. Several methods and techniques have been used to establish that the coordination number of the lighter ions (La^{3+} to Nd^{3+}) is predominantly nine, Gd^{3+} to Lu^{3+} are predominantly eight-coordinate species, and the aqua ions of Sm^{3+} and Eu^{3+} exist in an equilibrium between eight- and nine-coordinate species [70]. There have been several studies on the kinetics of water exchange on the Eu^{2+}(aq) ion and on several of its ternary complexes [77–79], prompted in part because it is accessible and secondly because it is isoelectronic with Gd(III), the latter being a key species in development of MRI contrast agents. Comprehensive accounts may be consulted regarding extensive work on the properties of ligands complexed with Gd(III), and the properties of the resulting complexes that render the species as suitable candidates for MRI agents [80–82]. In broad terms, the rates of exchange of the one or two water molecules in the coordination sites not occupied by the multidentate ligand need to be very high to provide the complex with high relaxivity, and the complex must possess a large stability constant. The latter

requirement is to reduce very significantly the concentration of free Gd^{3+} ions as they are toxic. Further reports on other multidentate ligands when complexed as potential MRI contrast agents and related aspects and properties may be consulted [83–89]. Thus, the experience gained initially of determining the kinetic parameters of water exchange on transition metal aqua ions and solvated transition metal complexes by NMR spectroscopy could be extended to the solvated lanthanide ions and to aqua-lanthanide coordination complexes, for a valuable medical application.

2.1.3. Kinetics of water exchange on hexa-aqua copper(II) and copper(II) complexes. The kinetics of water exchange on aquated Cu(II) ions were thought to be complicated by the consequence of Jahn–Teller distortion of the axial water molecules relative to the equatorial coordinated water molecules, assuming the aqua-ion is six-coordinate and octahedral. Octahedral geometry and six-coordination are generally considered to prevail in both the solid state and in solution. The latter was shown to be the case from neutron diffraction studies [90]. Kinetics measurements were reported in several publications, and the status of the subject up to 1990 was included in a publication in which inversion of the aqua-ion was determined to be much faster than water exchange between the aqua-ion and bulk water [91]. At 298 K the inversion time was cited as 5.1×10^{-12} s, whereas the water exchange rate constant, k_{EX}^{298K}, was $4.4 \times 10^{9}\,s^{-1}$, with $\Delta H_{EX}^{\#} = 11.5\,kJ\,mol^{-1}$ and $\Delta S_{EX}^{\#} = -21.8\,J\,mol^{-1}\,K^{-1}$. At that time the volume of activation could not be extracted from the primary data with certainty attached to the value, although it was declared to be a positive value. In a subsequent study [92], that included results for the kinetics of exchange of DMF on $Cu(DMF)_6^{2+}$ (DMF = dimethylformamide) with bulk solvent, an activation volume of $+2.0\,cm^3\,mol^{-1}$ was reported for water exchange on $Cu(H_2O)_6^{2+}$. It was noted that perhaps the negative entropy of activation would signify an expectation of a small negative volume of activation. Nevertheless, it was predicted that an I_d mechanism probably operates for water exchange. It was concluded that the time scale for inversion of the Jahn–Teller distortion axis on $Cu(DMF)_6^{2+}$ is similar to that for the hexa-aqua Cu(II) ion, and much shorter than the time scale for DMF exchange and rotation of the solvated complex. It prevailed that the volume of activation for DMF exchange on $Cu(DMF)_6^{2+}$ was $+8.4\,cm^3\,mol^{-1}$, a value strongly indicative of a dissociative activation mechanism, and in part a reflection of the greater bulk of the solvent ligand. In fact DMF exchange is characterised by a positive value even for $Mn(DMF)_6^{2+}$, whereas the smaller water molecule exchanges by an I_a mechanism on the hexa-aqua Mn(II) ion.

Thus a system, notably the kinetics and mechanism of water exchange on the hexa-aqua Cu(II) ion, that had occupied several investigating groups over a prolonged period of time seemed finally to be resolved unambiguously. However, a refined isotopic substitution method in a neutron diffraction study coupled with a first-principles molecular dynamics approach revealed that contrary to earlier accepted results the Cu(II) aqua ion exhibits five-fold coordination [93]. It was argued that earlier experimental data from visible, near infrared absorption and nuclear magnetic resonance spectroscopies as well as X-ray near edge structure determination could be rationalised to fit five-coordination. The simulations indicated that the solvated species undergoes frequent transformations between square pyramidal and trigonal bipyramidal configurations. The ^{17}O NMR spectroscopy data could be reinterpreted in terms of five-coordination and a slightly enhanced k_{EX} value of $5.7 \times 10^{9}\,s^{-1}$ was provided.

Soon after the appearance of the publication announcing the five-coordination state for hydrated Cu(II) ion, an extensive report on the coordination number and geometry of solvated Cu(II) ions in solution, and of the structure of Cu(II) complexes in the solid state also appeared [94]. These latest authors presented a detailed analysis and interpretation of crystallographic results from which regular octahedral coordination was indicated. They showed from a lattice-independent EXAFS study and with reference to electron spin resonance studies [95] that the local structure in the solid state Cu(II) complexes cited is consistent with a Jahn–Teller induced elongation, i.e. in effect, the equatorial/axial distortion coordination cannot be extracted from the crystallographic methods and data. Further analysis using EXAFS and large angle X-ray diffraction (LAXS) data upon the hydrated Cu(II) ion in aqueous solution modelled five- and six-coordination states. The combined results were consistent with a Jahn–Teller elongated octahedral configuration and distances of the copper–oxygen bonds for both equatorial and axial positions were obtained. Thus there remain different views on the coordination geometry and number of solvated Cu(II) ions. However, in another report arguments are made in favour of five-fold coordination [96].

There is little doubt though that when tetradentate tripodal ligands of the type shown in scheme 2 (for example, tren, (tren = 2,2′,2″-triaminotriethylamine), N-alkyl substituted tren, Me_6tren (Me_6tren = 2,2,′2″-tri(N,N-diethylamino)triethylamine), Me_3tren (Me_3tren = 2,2,2″-tri(N-monomethylamino)triethylamine), tmpa (tmpa = tris(2-pyridylmethyl)amine)), coordinate to Cu(II) in aqueous medium that the copper becomes five coordinate and the geometry is trigonal bipyramidal, with one water molecule in an axial position.

Early work on the kinetic and equilibrium properties of $[M(Me_6tren(H_2O)]^{2+}$ species, M = Ni, Co, Cu, had established the five-coordinate, trigonal bipyramidal geometry of such species [97]. Subsequent work from many sources and employing various techniques confirmed these findings, and some specific examples are cited below. The change in geometry diminishes Jahn–Teller distortion and therefore kinetic consequences ensue. There is a dramatic lowering of the rate of water exchange from that in the fully aquated Cu(II) ion. A study of the kinetics of water exchange, that was complemented by a study of the kinetics of substitution of water by pyridine and substituted pyridines on $[Cu(tren)(H_2O)]^{2+}$ demonstrated that the removal or significant reduction of Jahn–Teller distortion gave rise to a significant decrease (more than three orders of magnitude) in the lability of the coordinated water molecule [98]. The mechanism of water exchange was changed from that in the fully aquated Cu(II) ion (I_d) to I_a in $[Cu(tren)(H_2O)]^{2+}$. However, when six methyl substituents are present in the ligand, the water exchange rate in $[Cu(Me_6tren)H_2O]^{2+}$ is about a thousand times smaller again and the steric crowding effects a mechanistic changeover to I_d [99]. Yet the water exchange process on the Cu(II) complex of the trimethylated tren, (one methyl substituent on each original primary amine site) Me_3tren, $[Cu(Me_3tren)(H_2O)]^{2+}$, is characterised by a $\Delta V^{\neq}$ of $-8.7\,cm^3\,mol^{-1}$, indicating an I_a mechanism [100]. Other examples of rate retardation and mechanistic variation relative to properties of the aquated Cu(II) species are water exchange on $[Cu(tmpa)(H_2O)]^{2+}$ and on $[Cu(fz)_2(H_2O)]^{2+}$], (fz = ferrozine = 3-(-pyridyl)-5,6-*bis*(4-phenylsulphonic acid)-1,2,4-triazine), with $\Delta V^{\neq}$ values being -3.0 and $-4.7\,cm^3\,mol^{-1}$ respectively [101]. The latter complex is considered to possess square pyramidal geometry. Various other

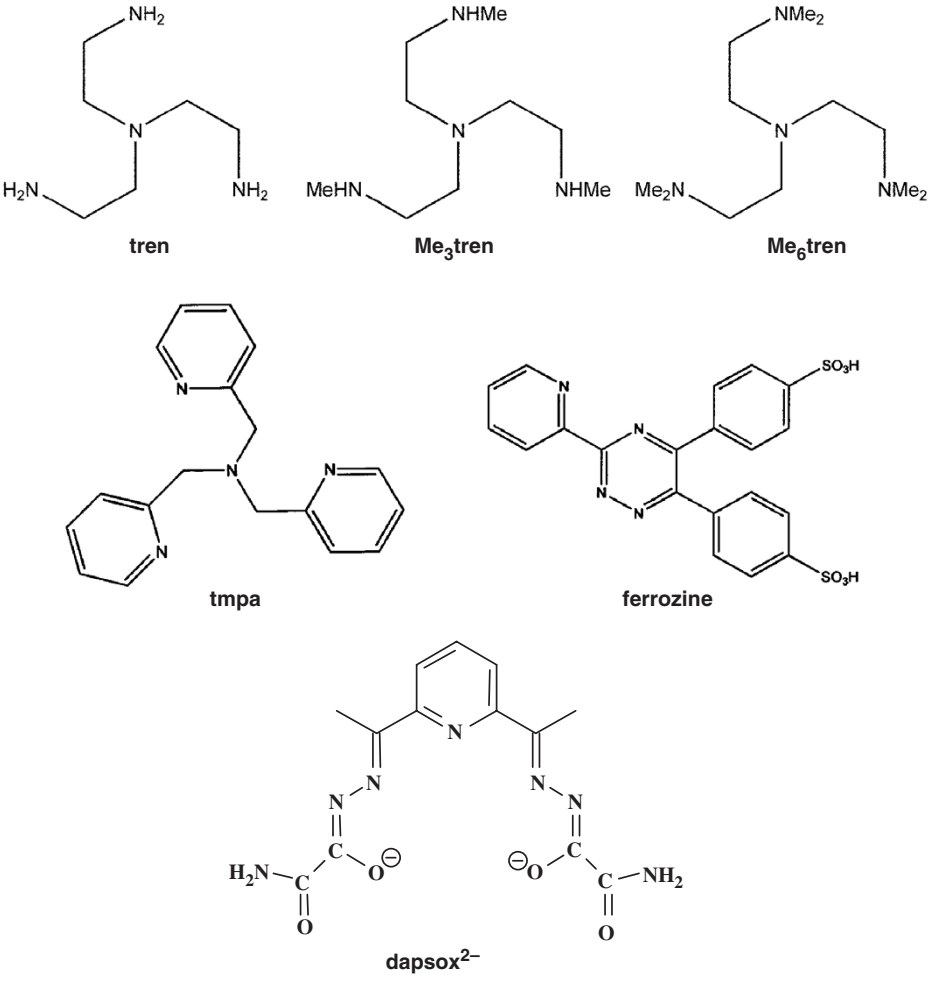

Scheme 2. Multidentate ligands.

aspects of these and related complexes are discussed as well in other literature [100]. Of additional interest are the kinetic parameters for water exchange on $[Cu(terpy)(H_2O)_2]^{2+}$ (terpy = 2,2′:6′,2″-terpyridine); they are k_{EX} (at 299.5 K) $= 6.6 \times 10^8\ s^{-1}$, $\Delta H^{\neq} = 20.7\ kJ\ mol^{-1}$, $\Delta S^{\neq} = -6.6\ J\ mol^{-1}\ K^{-1}$ and $\Delta V^{\neq} = 0.0\ cm^3\ mol^{-1}$ [102]. These were obtained employing ^{17}O NMR and esr line broadening methods. The exchange rate constant is thus only about one order of magnitude less than that for the aquated Cu(II) ion, although the coordination geometry of the complex was regarded as trigonal bipyramidal. But unlike the complexes cited earlier where the water molecule undergoing exchange is in an axial position, in this case the non-exchanging ligand is thought to occupy two axial and one equatorial position so the exchanging water molecules are in equatorial positions. The near zero entropy of activation and the zero volume of activation are consistent with an interchange (I) mechanism with neither bond-making nor bond-breaking dominating in the transition state.

2.2. *Ligand substitution reactions*

2.2.1. Solvent tuning of the kinetics of ligand substitution of a seven-coordinate iron(III) complex. Knowledge of the solution properties and mechanism of substitution of seven-coordinate 3d metal complexes is scarce. The most recent report [103] of a series of studies [104–106] on the reactivity of the pentagonal bipyramidal complex $[Fe(dapsox)(L)_2](ClO_4)$, (H_2dapsox = 2,6-diacetylpyridine-*bis*(semioxamazide), L = solvent or its deprotonated form), (see scheme 3) in different solvents, illustrated that rather than a medium effect alone, substitution of solvent by SCN^- affected marked changes in mechanism. In addition to the importance of fundamental reactivity studies on this complex (see structure of the diaqua complex), relevance to the catalytic cycle of superoxide dismutase has been established. In water, methanol and ethanol, and in acidified methanol and ethanol, the substitution of both axial solvent molecules can be characterised kinetically, whereas in DMSO substitution of only one coordinated DMSO by SCN^- could be characterised. Without acidification of alcohol solutions one of the bound alcohol molecules is deprotonated.

A general reaction scheme for the first step is:

$$[Fe(dapsox)(L)_2]^+ + SCN^- \rightleftarrows \{[Fe(dapsox)(L)_2]^+ \cdot NCS^-\} \quad K_{os} \tag{5}$$

$$\{[Fe(dapsox)(L)_2]^+ \cdot NCS^-\} \rightleftarrows [Fe(dapsox)(L)(NCS)] + L \quad k_1, k_{-1} \tag{6}$$

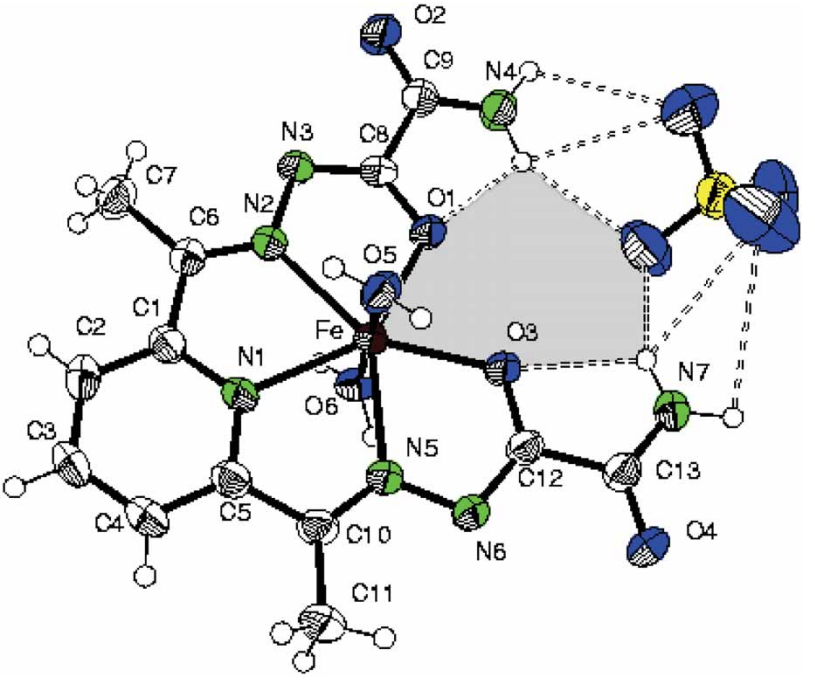

Scheme 3. Structure of the diaqua Fe^{III}(dapsox) complex. The structure of the dapsox ligand is included in scheme 2.

where K_{OS} represents the equilibrium constant for outer-sphere precursor formation, and k_1 and k_{-1} are the forward and reverse rate constants for ligand interchange. A rate law could be developed from this scheme, and applying conditions relative to each reaction, and using approximations and estimates for the effect of pressure on K_{OS}, the thermal and pressure related activation parameters could be extracted. It prevailed that except for the reactions in acidified alcohols and in DMSO there was no evidence of a reverse reaction. The second-order rate constant was higher in ethanol than in methanol, and in turn higher than in water, a reflection of the strong *trans* effect of the axially coordinated ethoxo ligand and high lability of the ethanol molecule in the *trans* position. The enthalpies generally mirrored the reactivity trend, and the entropies of activation were markedly positive. The volumes of activation were distinctly positive in both alcohols and after allowing for the contribution of $\Delta V(_{OS})$ indicated a dissociative (D) mechanism. This is in contrast to the I_a mechanism proposed from interpretation of the activation parameters for reaction in acidified ethanol and methanol, water and DMSO. Substitution in the latter media is much slower than in the alcohol solutions in which one coordinated solvent is deprotonated, affecting the charge. Interestingly at higher pH, in aqueous solution, the first substitution occurs by a dissociative interchange mechanism as a result of the *trans* effect of the hydroxo ligand.

Substitution by a second SCN^- in some cases was significantly slower enabling the rate constants to be extracted from the spectrophotometric primary data, whereas in other circumstances a solution containing primarily the monosubstituted Fe(III) complex was reacted with a solution of SCN^- to obtain the kinetic parameters. These could be analysed to show that the second substitution always proceeds by an I_d or D mechanism. These remarkable reactivity and mechanistic differences are a result of the axial coordinated solvent molecules. Finding that some reactions proceed by an I_a mechanism was an unexpected result since the complex is seven-coordinate. This feature was discussed in the context of related reactions of Fe(II) complexes.

The reversible first substitution reactions in acidified methanol or ethanol could be characterised in both directions as a function of hydrostatic pressure, decelerating and accelerating in the forward and reverse reactions with increasing pressure, respectively. The observed $\Delta V^{\neq}$ for the forward reaction is a composite value made up of a positive value arising from charge neutralisation in the precursor complex formation, (lowered electrostriction) and a negative contribution from the associative interchange mechanism of the actual rate-determining substitution step. Overall it is a small positive value. The reverse solvolysis reaction is between two neutral species and solvent electrostriction changes are not thought to contribute significantly. Thus the negative value of $\Delta V^{\neq}$ is a consequence of the associative interchange mechanism. For the first step of the substitution reaction these volume changes are neatly illustrated in a volume profile (see figure 1).

2.2.2. Formation of terpyridine complexes from aqua-ions of Co(II), Ni(II), Cu(II) and Zn(II). A combination of results of studies of the kinetics of reactions of aqua ions of Co(II), Ni(II) and Zn(II) with 2,2′-bipyridine (bpy), 1,10-phenanthroline (phen) and terpy, and of the kinetics of solvent exchange led to the formulation of the Eigen–Wilkins mechanism [12, 23, 107]. Several other reports at the time [12, 23, 108, 109] led to the assessment that a coherent mechanistic picture was unfolding. In the case of the reaction of Ni(II) the substitution of water by terpy in $[Ni(terpy)(H_2O)_3]^{2+}$ was found to

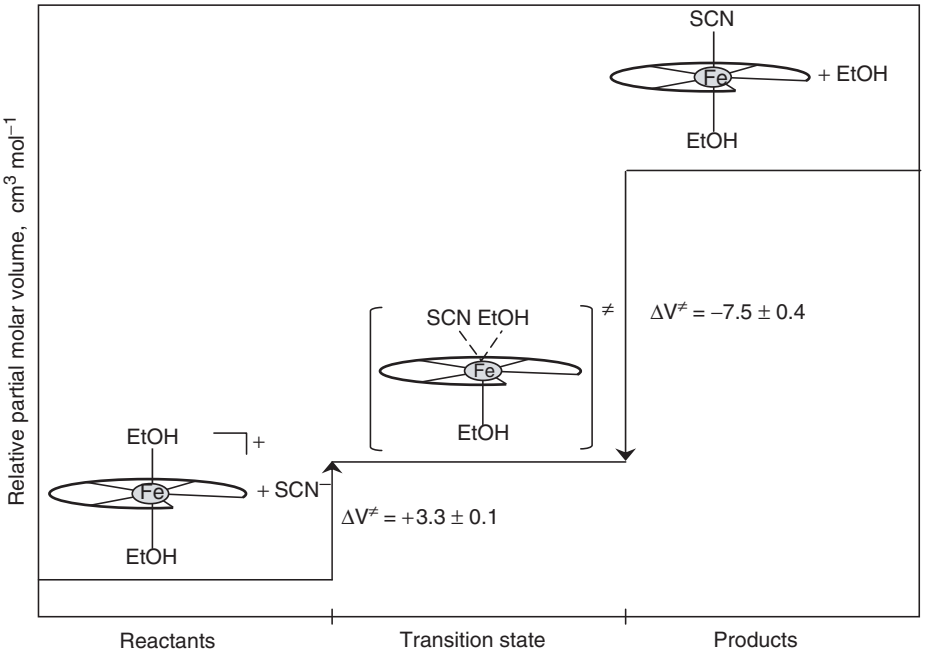

Figure 1. Volume profile for the first reaction step between $[Fe(dapsox)(EtOH)_2]^+$ and SCN^- in acidified EtOH.

be about 200 times faster than the formation of the mono(terpy) complex. Since the rate of water exchange on the mono complex was very similar to that on the aqua nickel(II) ion [110], it was argued that a favourable interaction between the incoming terpy ligand and the terpy of the mono complex caused a significant increase in the outer-sphere equilibrium constant [110]. In these kinetic studies in aqueous solution it was implied that in the *bis* complex there were four chelate rings. Subsequent studies using the solvates of Co(II), Ni(II), Cu(II) and Zn(II) in kinetics experiments applying multi-wavelength sf spectrophotometry using terpy and several substituted terpy ligands have revealed some interesting coordination chemistry features [102]. When excess Co(II), Ni(II) or Zn(II) are used in reactions with terpy, intermediates are observed prior to the formation of the mono(terpy)metal(II) complex. The kinetics results were consistent with formation of a complex species in which the terpy is bound as a bpy-type bidentate ligand, and this is followed by a chelate-ring closure step. An estimate of the equilibrium constant for the intermediate was a value expected for a bidentate, but not a terdentate complex species and thus supported the analysis of the kinetics results. When $Cu(aq)^{2+}$ reacts with excess terpy at pH 6.1 (buffered with MES = 4-morpholineethane-sulphonic acid) several steps were observed. The initial formation of mono(terpy)Cu(II) is followed by rapid formation of five-coordinate *bis*(terpy)Cu(II) intermediates, with the second terpy serving as a bidentate ligand, and subsequently slow rearrangements of these intermediates occur. The final complex species was thought to be $[Cu(terpy)_2]^{2+}$, and various possible species were suggested to be formed, but further work was said to be required in order to unravel all the complications. While these findings may seem inconsistent with the earlier work, the later reactions relating to

the copper species were carried out in MES buffer whereas previously the aqueous medium was pH controlled, but not with buffer materials present. The later reactions of Co(II), Ni(II) and Zn(II) were carried out in 80% methanol: hence it is not clear that the transition states are the same when the media are very different. A following report aimed to illuminate further the reason why the *bis*(terpy)Ni(II) complex is formed much more rapidly from the mono(terpy)Ni(II) complex than is the latter from aqua-Ni(II) and terpy [111]. The kinetics of seven different substituted terpy ligands reacting with $Ni(terpy)^{2+}$ were investigated and a rate enhancement factor for each one relative to the rate constant for formation of the mono(terpy)Ni(II) complex was obtained [112]. The substituents were mostly on the 4-position of the central pyridine moiety and included, phenyl, pyridyl, naphthyl, tolyl and t-butyl-phenyl. The ligands were designed in an attempt to examine whether the "stacking" effect invoked to increase the outer-sphere pre-equilibrium constant could be understood in more detail. There were some surprises in the rate enhancement values, for example the value for the pyridyl substituent was less than that for the 4-phenyl substituted ligand. No totally clear pattern emerged even after the geometric possibilities of interactions had been explored. However, it was concluded that stacking interactions are important and the rate-determining step in the expulsion of solvent molecules must occur early, during the first metal-ligand bond formation, and that a ring closure step would not be compatible with the observations. The solvent composition was chosen as a compromise (65% : 35% methanol : water) for sufficient solubility yet still allowing the remaining coordination sites on Ni(II) to be solvated by water. However, the rate enhancements were predicted to be lower, and were found to be lower than if water alone was the solvent, owing to the medium difference imposed. The estimates of the stacking contributions were consistent with similar interactions measured in other systems [113].

2.2.3. Ligand substitution at aqua-ruthenium(III)(edta). It has become apparent that complexes of edta with Ru(III) may offer scope for potential application in biologically relevant models [114]. Thus knowledge of the species present and their concentration distribution at equilibrium when $[Ru^{III}(edta)(H_2O)]^-$ reacts with amino acids or thiols containing an additional functional group can provide suitable fundamental information, for example for designing kinetics experiments for the same reactions. Reactions of glycine, L-cysteine and S-methyl cysteine with $[Ru^{III}(edta)(H_2O)]^-$ were characterised kinetically [115]. Each showed a rapid amino acid concentration-dependent complex-formation of $[Ru^{III}(edta)(am)]^-$ (am = amino acid), followed by a slow am concentration-independent ring-closure step. It was noted that the initial ruthenium complex inhibits cysteine protease activity in papain and bromelain. A subsequent similar study employed 2-mercaptoethanol, mercaptoacetic acid, methylthioglycolate and 2-aminoethanethiol as the substituting ligands [116]. In each case a rapid reaction occurred, and under pseudo first-order conditions (thiol in excess of the ruthenium complex concentration) the first-order rate constant depended linearly on the thiol concentration and no reverse aquation reaction was detected. The second-order rate constants were all within a factor of two of one another, meaning that possible interactions with the uncoordinated carboxylate group of edta that explain the faster reactions, are minor in terms of the magnitude of the Gibbs energy of activation. A second slower step was detected in the reactions of mercaptoacetic acid and mercaptoacetate, and the first-order rate constants were independent of thiol concentration. The temperature and

pressure dependencies of the kinetic parameters of the faster step gave rise to the activation parameters, $\Delta H^{\neq}$ of about $40\,kJ\,mol^{-1}$, $\Delta S^{\neq}$ in the range -50 to $-70\,J\,mol^{-1}\,K^{-1}$ and $\Delta V^{\neq}$ in the range -5 to $-9\,cm^3\,mol^{-1}$. Overall the results can be interpreted as an associatively activated rapid substitution reaction to form a mono-coordinated (S-donor atom) complex through substitution of coordinated water. This is followed by a ring-closure step (independent of thiol concentration) in two cases, where the carboxylate group in mercaptoacetic acid or the acetate group coordinates to the metal centre by displacing one carboxylate arm of the edta ligand. No second step was observed in the reaction of mercaptoethylamine as the amino group that would close the chelate ring is protonated under the conditions of the experiment. In the case of the reaction of mercaptoethanol, hydrogen bond formation between the ligand and the unbound carboxylate was invoked to explain the absence of a detectable second reaction step.

2.2.4. Substitution at square planar platinum(II)

2.2.4.1. Nucleophilic substitution on $[Pt^{II}(N\text{-}N)(H_2O)_2]^{2+}$ complexes. Substitution in square planar complexes, mostly Pt(II) complexes, represents a wide ranging field of endeavour that has been ongoing for sometime. The finding that [*cis*-$Pt(NH_3)_2Cl_2$], cisplatin, possesses anti-tumour activity stimulated development of other Pt(II) complexes that might provide higher chemotherapeutic efficacy. A comprehensive description of the discovery and development of cisplatin has appeared recently [117]. The chemistry involved in the activity is complicated and many reaction steps are feasible. These include aquation, ligand substitution, transformation reactions with proteins, DNA, or components thereof, of cisplatin, and the pH dependencies of these processes. Therefore, establishing the properties of various Pt(II) complexes that may reasonably satisfy the criteria as a potential medicinal agent has attracted considerable research effort. The properties of spectator ligands, for example a π-acceptor, and whether they are bidentate or terdentate, the significance and appropriate properties of S-containing nucleophiles for ligand substitution reactions in Pt(II) complexes and other relevant considerations have been thoroughly presented [118]. Earlier work had examined mono-functional Pt(II) complexes containing terdentate ligands, for example terpy, in a kinetics study and trends in reaction rates, pK_a values and nucleophilic discrimination were dependent markedly on the π-acceptor properties of the spectator ligands [119]. Arguments were presented to indicate that a bidentate spectator ligand possessing suitable properties could serve as the basis for a study of the reactivity of Pt(II) complexes toward substitution by thiourea, (tu,) L-methionine (L-Met) and guanosine-5′-monophosphate (5′-GMP^-). The dichloro complexes of Pt(dach), Pt(en), Pt(amp) and Pt(bpy) were prepared and the kinetics of substitution of the two coordinated water molecules, formed upon aquation, were studied as a function of nucleophile concentration, complex concentration, temperature and pressure. Pt(dach) is $[Pt(diaminocyclohexane)(H_2O)_2]^{2+}$, Pt(en) is $[Pt(ethenediamine)(H_2O)_2]^{2+}$, Pt(amp) is $[Pt(aminomethylpyridine)(H_2O)_2]^{2+}$ and Pt(bpy) is $[Pt(N,N'\text{-bipyridine})(H_2O)_2]^{2+}$ (see scheme 4). The rationale for choice of ligands resided in bifunctional characteristics employing a mixed amine/pyridine combination or two amine or two pyridine moieties in each bidentate.

For each complex the pK_a values of the coordinated water molecules were determined by means of spectrophotometric titrations. This enabled the selection of pH for kinetics

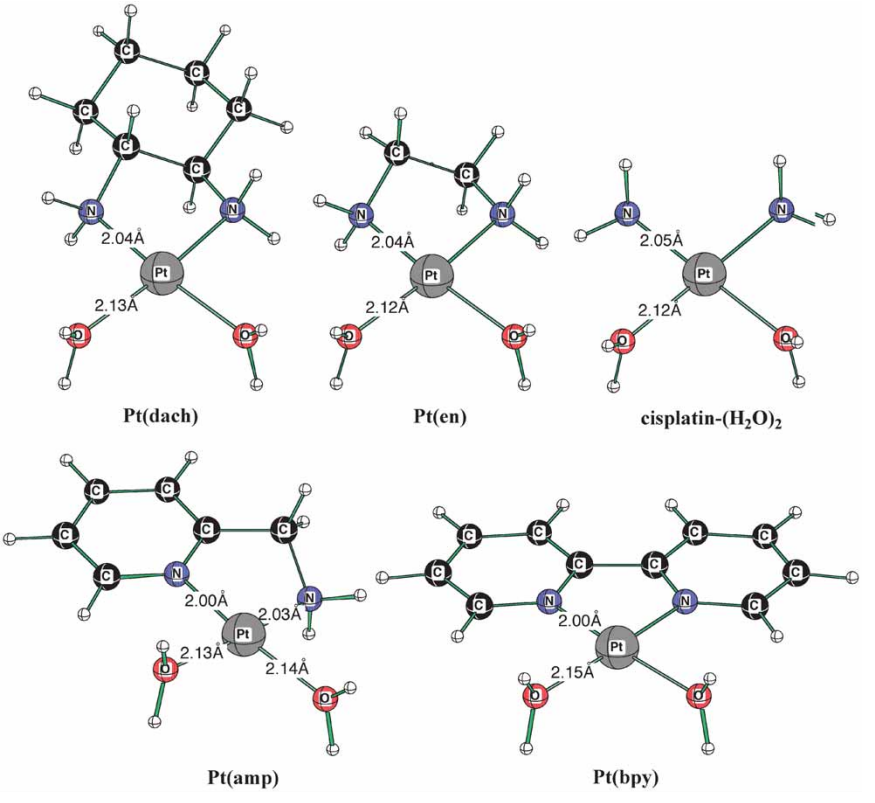

Scheme 4. Model Pt(III) complexes.

experiments that eliminated complications from OH-bridged or dihydroxy Pt(II) complex species. Substitution occurs in two distinct reaction steps, corresponding to the successive removal of the water molecules, but with L-Met functioning as a chelating ligand as the second water molecule is substituted. The first water molecule removal by L-Met is accompanied by S-coordination, followed by N-coordination as the chelate ring closes. This aspect of the reaction of L-Met was detected from the nucleophile concentration-independence of the rate constant for the second step. The primary kinetic data can be treated to show that the reactions are essentially irreversible, and therefore the kinetics observations do not contain a contribution from the reverse, aquation reactions. The order of reactivity for a given complex for the first step is tu > 5′-GMP > L-Met reflecting tu as the strongest nucleophile. Indeed after substituting two water molecules, tu labilises the Pt–N bond in the *trans* position to form a ring-opened trisubstituted species, $[Pt(tu)_3(N\text{-}N_{open})]^{2+}$. The rate constants for the second step would not be expected to correlate with nucleophilic strength, as the mono-substituted complex presents a different stereochemical species to the second incoming nucleophile, and in the case of L-Met the second step is not addition of a second ligand. The results demonstrate that π-acceptors increase the electrophilicity on the Pt(II) metal centre, owing to their electron-withdrawing property, which results in increasing rates of nucleophilic substitution. This is aptly illustrated by the fact that when the two

pyridine rings are adjacent to each other as in Pt(bpy) the rate increases by a factor of about 30–150 relative to Pt(dach)/Pt(en). The rate enhancement factor is in the range 3–7 when only one π-acceptor is present, as in Pt(amp). The trend in reactivity is mirrored in the activation enthalpies, as the higher electrophilicity of the metal centre stabilises the transition state and lowers the activation enthalpy. The values of the activation entropy and the activation volume are all significantly negative, indicating an associative substitution mechanism and an activation process dominated by bond formation. In the case of the chelate ring closure step in the reaction of Pt(en) with L-Met, the experimental value of $\Delta V^{\neq}$ of $-24\,cm^3\,mol^{-1}$ required a correction for the fact that a proton is liberated upon chelation; an estimate of the volume contribution of the latter process resulted in a value of between -16.3 and $-19.8\,cm^3\,mol^{-1}$ for associative ring-closure of coordinated L-Met. Overall the results illustrate that the nature of the N–N chelate has a marked influence on the pK_a values and substitution rates of the complexes studied: the significance of this fundamental information for developments of new active compounds was indicated. Various calculations by Density Functional Theory (DFT) were made in support of some of the subtleties of aspects of this project, including calculated structures of the complexes and that of cisplatin [118].

2.2.4.2. Substitution reactions of ternary Pt(II) complexes with biologically relevant ligands. A series of publications has appeared that complements the previous subsection. These include the kinetics of reaction of $[Pt(terpy)(H_2O)]^{2+}$ with S-donor ligands, the substitution reactions of $[Pt(terpy)(H_2O)]^{2+}$, $[Pt(terpy)(S\text{-cyst})]^{2+}$ and $[Pt(terpy)(N7\text{-guo})]^{2+}$, where S-cyst is L-cysteine and N7-guo is guanosine, with biologically relevant ligands and the competitive reactions of 5′-GMP and GSH (GSH = glutathione) with $[PtCl(terpy)]^+$ [119–123]. The multiplicity of studies can be seen to be aimed at establishing a wide array of kinetic and equilibrium properties of complex species, ligands and reaction conditions that form a data base for designing alternative models for cisplatin or co-administration agents. In this regard, the latest report includes a useful schematic of known and probable events in a cascade of relevant reactions [124]. A study of the complex formation kinetics of $[Pt(dien)(H_2O)]^{2+}$, $[Pt(dien)Cl]^+$ and $[Pt(dien)Br]^+$ (dien = diethylenetriamine) with inosine, (INO), inosine-5′-monophosphate (5′-IMP), 5′-GMP, GSH and L-Met in aqueous medium has been undertaken [124] (see scheme 5).

^{1}H NMR spectroscopic and UV-Visible spectrophotometric techniques were employed. The second-order rate constants for substitution of H_2O, Cl^- or Br^- showed that of the incoming nucleophiles L-methionine is the most effective and water is the most readily substituted. Variations among the rates for the other ligands whether S-bonding or N-bonding were discussed. The entropies of activation were all markedly negative and indicated an associatively activated reaction mechanism. In the complex set of possible transformations in Pt-based drug treatment, ligand substitutions, involving S-donor ligands may occur. To develop an understanding of these a competitive reaction between L-methionine and guanosine-5′-monophosphate for $[Pt(dien)Cl]^+$ was monitored by ^{1}H NMR spectroscopy. Formation of $[Pt(dien)(S\text{-met})]^{2+}$ occurred rapidly, but subsequently the S-donor ligand was replaced, very slowly, by 5′-GMP, to yield $[Pt(dien)(N7\text{-GMP})]^{2+}$.

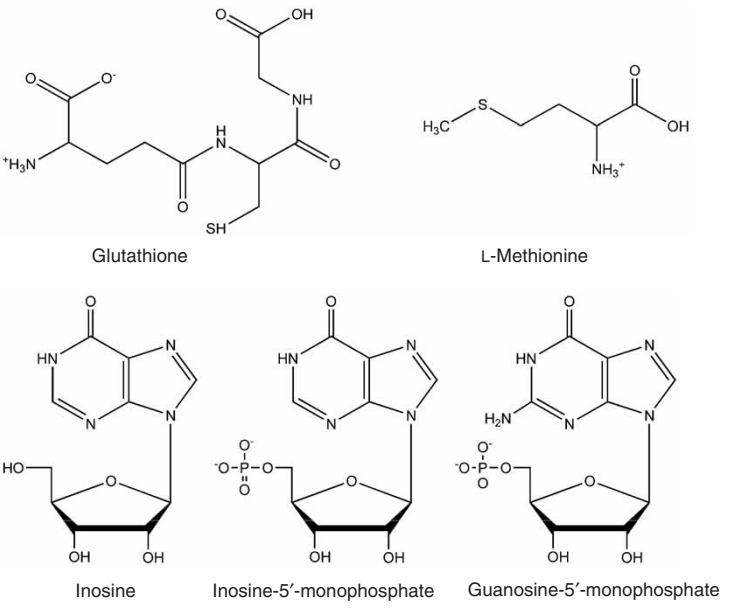

Scheme 5. Nucleophiles used for reaction with Pt(II) complexes.

2.2.4.3. Solvent effects on nucleophilic substitution reactions of $[Pt^{II}(L^3)Cl]^+$ complexes. Recently, as noted earlier, it was shown that for ligand substitution for a series of (aqua)Pt^{II}(terdentate) complexes in which the number of π-acceptor ligands varied, the π-acceptor effect controls the substitution rate, thought to be caused by a decrease in electron density and an increase in the electrophilic character of the metal centre. The medium in which platinum-based therapeutic agents may function can vary. Accordingly a study of how the π-acceptor effect on ligand substitution reactions at related Pt(II) complexes manifests itself in different solvents has been performed [125]. The selected nucleophile was tu and since the complexes reacted were chloro complexes the overall reaction involves charge creation, viz.

$$[Pt(L^3)Cl]^+ + tu \rightarrow [Pt(L^3)tu]^{2+} + Cl^-. \quad (7)$$

The complexes and their abbreviations are shown in scheme 6.

The solvents chosen were formamide, water, methanol, ethanol, 1-propanol and 1-pentanol to provide a range of dielectric constant from 14 to 110. In one or two cases the measurement of the kinetics of substitution was thwarted by formation of colloidal particles or solubility limitations. Where the reactions could readily be studied the dependence on excess tu concentration of the pseudo first-order rate constants was linear and no evidence of a reverse reaction was found. For reactions in methanol and water the rate constant correlated with the solvent polarity, whereas the rate constants for the alcohol solvents increased with increase in the carbon chain length of the alcohol. This latter finding, perhaps unexpected, was explained as possibly arising from van der Waals forces of the increasing carbon chain stabilising the transition state.

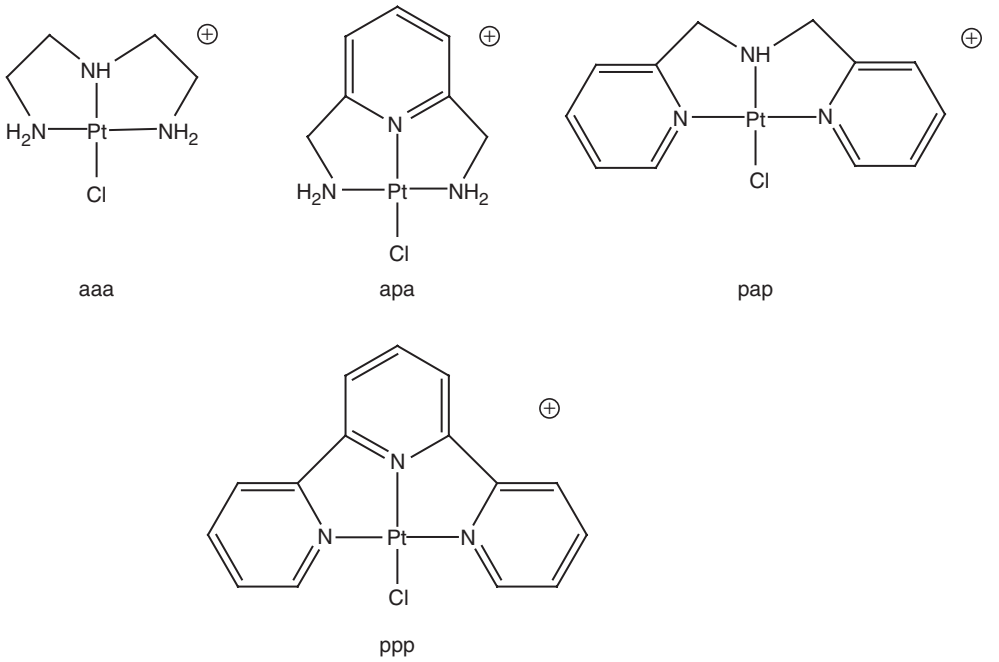

Scheme 6. Terdentate-chloro-Pt complexes.

The effect of π-acceptor ligand moieties was most dramatically illustrated by contrasting the second-order rate constants for the substitution reaction in water. They were at 298 K, $2.80 \times 10^3\,mol^{-1}\,dm^3\,s^{-1}$ for ppp, 3.67 and $1.63\,mol^{-1}\,dm^3\,s^{-1}$ for pap and apa respectively, and $0.538\,mol^{-1}\,dm^3\,s^{-1}$ for the reaction of aaa. Similar dramatic rate enhancements were observed for the substitution reaction of the complex containing the three pyridine donors of ppp, in the other solvents. The activation parameters were obtained for reactions in methanol and water. The entropies and volumes of activation were all negative, and the former were all more negative in water, results ascribed to more structuring of water around the transition state compared to the number of methanol molecules structured around the transition state. In the case where $\Delta V^{\neq}$ could be obtained for comparison, it was more negative for the reaction (of apa) in water than the reaction in methanol. As could be predicted the values of $\Delta H^{\neq}$ were lower for the faster reaction in water, than the values of the same parameter for reaction in methanol, for a given complex.

2.2.2.4. Substitution reactions of [Pt(bmpa)(H$_2$O)]$^{2+}$ and [Pd(bmpa)(H$_2$O)]$^{2+}$. The overall studied reaction is:

$$[M(bmpa)(H_2O)]^{2+} + L \rightleftarrows [M(bmpa)L]^{2+/1+} + H_2O. \quad (8)$$

M = Pd(II) or Pt(II); L = tu, dmtu, tmtu, Cl^-, Br^-, I^- or SCN^-; bmpa = *bis* (2-pyridylmethyl)amine. (dmtu = dimethylthiourea; tmtu = tetramethylthiourea)

One principal objective of this study [126] is a determination of the effect of different nucleophiles (Nu) on the reactivity of a given metal complex. In addition, comparisons of the effect of bmpa as a terdentate ligand (relative to other coordinated terdentate

ligands in similar substitution reactions) and of the relative reaction rates of substitution of the Pt- and Pd-complexes were probed. Complexes of Pd(II) are normally much more labile than the corresponding complexes of Pt(II). This property was confirmed in this study. The rate law is ($k_{obs} = k_2$[Nu], where k_{obs} = pseudo-first-order rate constant, k_2 = second-order rate constant, and no evidence of a reverse reaction was detected. The derived second-order rate constants for nucleophilic substitution were about 10^3 higher for the Pd(II) complex. However, this rate difference is less than the 10^5–10^6 factor usually encountered [127] and may be explained as a consequence of π-back bonding from the two *cis*-pyridyl rings to the softer platinum centre. The reactivity of the nucleophiles towards the complexes followed the order tmtu < tu < dmtu for $[Pt(bpma)(H_2O)]^{2+}$ and tmtu < tu ≈ dmtu for $[Pd(bpma)(H_2O)]^{2+}$. Based upon steric considerations alone tu would be expected to react more rapidly, but the inductive effect of the two methyl groups in dmtu appears to render the latter a stronger nucleophile while the steric effect appears to dominate in the reactivity of tmtu. For the palladium complex the inductive effect is less significant owing to the nature of the metal centre. The reactivity of the anionic nucleophiles followed the order $I^- > SCN^- > Br^- > Cl^-$, an order that depends upon the polarisability of the incoming ligand and the softness or hardness of the metal. The iodide ion being the most polarisable reacts much faster than the other nucleophiles. The π-back bonding effect that labilises substitution in $[Pt(bpma)(H_2O)]^{2+}$ is an effect found also in the reaction of $[Pt(terpy)(H_2O)]^{2+}$ complexes with thiols. The sensitivity of the rates of reaction to different nucleophiles and the significantly negative entropies of activation support the expectation that the mechanism is associative.

At the conclusion of the sub-topic of kinetics of ligand substitution reactions at Pt(II) it should be emphasised that there are countless other studies centred upon coordination complexes of other metals where the search for alternative compounds that could imitate the favourable characteristics of cisplatin, but do not possess the unfavourable aspects of cisplatin, in its therapeutic role. Some examples of relevant studies of kinetics of ligand substitution are Pd(II) complexes [128, 129], Rh(III) species [130] and Ru(III) complexes [131].

2.2.5. Kinetics of lanthanum(III) complexation of acetohydroxamic acid. Studies of the kinetics and mechanism of solvent exchange on La(III) ions are abundant as noted in section 2.1.2. Corresponding studies on formation of complexes of lanthanide elements (in oxidation state +3) are relatively uncommon. A complicated reaction set in which ternary aqua-La(III) complexes of tetraazamacrocyclic ligands bearing pendant arms react with oligonucleotides and other model DNA species has been reported [132]. It appears that the rate constants for these reactions are controlled by the rate of displacement of the water ligands, which themselves may be controlled by steric constraints arising from the bulky pendant arm substituents. The kinetics of formation of La(III) complexes of *trans*-1,2-diaminocyclohexane-N,N,N′,N′-tetraacetate and of cyclen derivatives bearing two or three $CH_2CO_2^-$-derivatised pendant arms have also been investigated [133, 134].

The La(III) ion forms stable complexes with hydroxamic acids [$R^1C(=O)N(OH)R^2$], coordinating through the two oxygen atoms accompanied by release of one proton. Hydroxamic acids can exist in *cis* and *trans* forms, but obviously only coordinating in the *cis* form. It was proposed that a slow *trans* to *cis* isomerisation of

N-alkylhydroxamic acids was the rate-determining step for their chelation to La(III) ions [135]. Yet when $R^2 = H$ (=HA), the complexation rate was very rapid. Accordingly ^{139}La NMR spectroscopy was employed to study the complex formation of La^{3+} with HA ($R^1 = CH_3$; $R^2 = H$) in aqueous solution [136]. From considerations of the properties of the system it could be argued that the reactions that are responsible for the observations are

$$La^{3+} + HA \rightleftarrows La(A)^{2+} + H^+ \quad k_{11}, k_{-11} \tag{10}$$

$$La^{3+} + A^- \rightleftarrows La(A)^{2+} \quad k_{12}, k_{-12}. \tag{11}$$

Rate constants for the forward reactions, k_{11} and k_{12} were obtained, while the parameters for the reverse reactions were obtained from the former and the magnitudes of the equilibrium constants, also obtained in this study. Although the authors pointed to the difficulties in proceeding from primary data acquisition to obtaining thermal activation parameters, they were able to conclude from the distinctly positive entropies of activation that the forward reactions are dissociatively activated. Since k_{11} and k_{12} were not of similar magnitudes it could be concluded that a rate limiting chelation step could not be limited by *trans* to *cis* isomerisation. In fact it was determined that the isomerisation rate constant for HA exceeds that for N-alkyl derivatives by at least a factor of 10^5.

2.3. *Redox reactions*

2.3.1. Electron transfer reaction between phenothiazines and hexaaquairon(III). Phenothiazines are a class of compounds of pharmacological value [137]. Among their properties is the ability to undergo one electron-transfer reactions [138]. Early work established that the electron-transfer ability varied with the N-alkyl substituent [139]. Kinetic studies of the reactions of both promazine, (dimethyl-(3-phenothiazin-10-yl-propyl)-amine), and promethazine, (dimethyl-(2-phenothiazin-10-yl-propyl)-amine), with hexaaquairon(III) (see scheme 7), as a function of hydrostatic pressure have been conducted in order to illuminate further the factors that determine the similarities and differences in related reactions [140, 141].

For the reaction of promazine with hexaaquairon(III) the volumes of activation for the forward reaction and reverse reaction were determined to be -6.2 and $-12.5\,cm^3\,mol^{-1}$ respectively meaning that the transition state has a smaller partial molar volume than that of either reactants or products. A general reaction scheme can be written,

$$\text{Phenothiazine} + Fe^{3+}_{(aq)} \rightleftarrows \text{phenothiazine}^{+\cdot} + Fe^{2+}_{(aq)} \quad k_f, k_r \tag{12}$$

and the phenothiazine product is a cation radical species.

In order to determine whether the kinetic and activation parameters lead to a similar profile of volume changes, the reaction of promethazine with hexaaquairon(III) was investigated as a function of pressure. However, as the equilibrium was unfavourable from the point of view of studying the reaction in the forward direction, the reaction

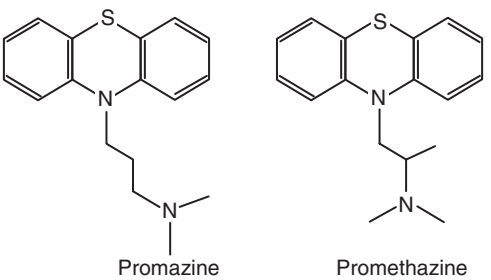

Scheme 7. Phenothiazines.

was studied in the reverse direction, reacting hexaaquairon(II) with the promethazine radical, in perchloric acid. An excess of both iron species over promethazine concentration converts the reversible second-order reactions (established earlier) into pseudo-first-order processes. The pseudo-first-order rate constant, k_{obs} can then be expressed as

$$k_{obs} = k_f[Fe^{III}] + k_r[Fe^{II}]. \quad (13)$$

The relationship between k_{obs} and $[Fe^{II}]$ was linear, and permitted the determination of k_f from the intercept and k_r from the slope at each applied pressure. The volumes of activation, $\Delta V^{\neq}(k_f) = -6.2$ and $\Delta V^{\neq}(k_r) = -11.4\,cm^3\,mol^{-1}$, respectively are remarkably close to those obtained for oxidation of promazine and suggest that solvation and any intrinsic volume changes are very similar for the two reactions. The reaction volume of $+5.2\,cm^3\,mol^{-1}$ could be obtained as well from the pressure-dependence of the system in equilibrium. The kinetically determined value was confirmed by an identical value of the reaction volume obtained from the pressure dependence of the equilibrium constant. The reduction of $Fe^{3+}_{(aq)}$ to $Fe^{2+}_{(aq)}$ is accompanied by a volume increase of $13.6\,cm^3\,mol^{-1}$, $+4\,cm^3\,mol^{-1}$ of which is a consequence of a solvational effect and the remaining $+9.6\,cm^3\,mol^{-1}$ arises from intrinsic changes [142]. It therefore follows that the reaction volume change associated with oxidation of promethazine should be about $-8\,cm^3\,mol^{-1}$. From crystallographic data and other information it could be argued that intrinsic volume changes upon oxidation of promethazine would be minor, and thus the electrostrictive contraction of solvent molecules upon forming the charged cation radical is the principal contributor to this component of the reaction volume.

The volume profile (see figure 2) for oxidation of promethazine based on the quoted volumes of activation shows again a more compact transition state, and this suggested a precursor contact pair forms in both directions of the reaction. It was also suggested that the more negative volume of activation for the reverse reaction is a result of a larger change in electrostriction relating to charge concentration in the precursor complex or the transition state.

Application of Marcus–Hush theory to this outer-sphere electron-transfer reaction [143, 144] permitted the calculation of the volume of activation ($-6.5\,cm^3\,mol^{-1}$) for the promethazine/promethazine$^{+\cdot}$ self-exchange reaction [145–147]. This value is close to the value of the volume of activation for the forward reaction, and the value for the self-exchange volume of activation ($-11.4\,cm^3\,mol^{-1}$) of the Fe^{2+}/Fe^{3+} couple is close to that for the reverse reaction. It is, therefore, evident that the volume change in the

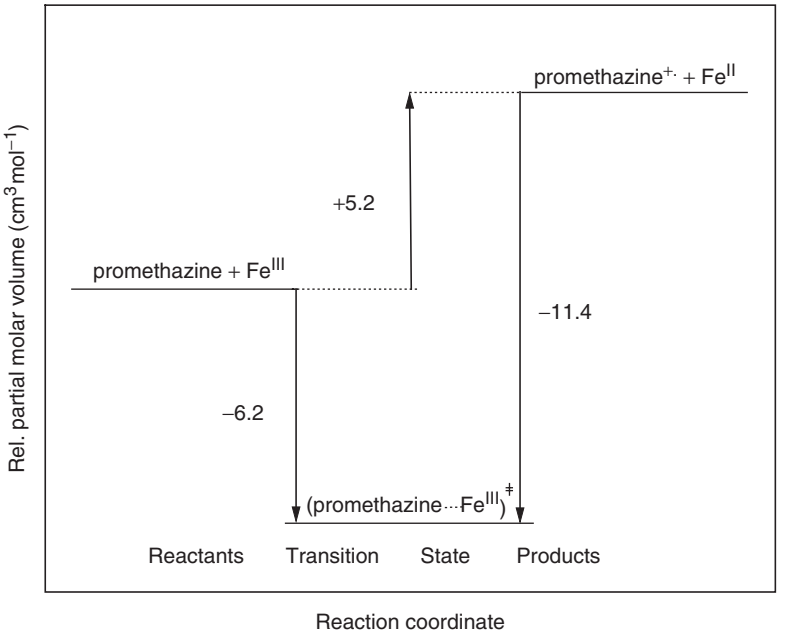

Figure 2. Volume profile for the reaction

$$\text{Promethazine} + Fe^{3+}_{(aq)} \rightleftarrows \text{Promethazine}^{+\cdot} + Fe^{2+}_{(aq)}.$$

forward reaction is dominated by the electrostriction change upon forming the cation radical of promethazine. The volume of activation of the reverse reaction is dominated by the electrostriction change upon oxidation of $Fe^{2+}_{(aq)}$. These redox reactions provide an excellent illustration of the power of application of hydrostatic pressure in a kinetics investigation in obtaining fine detail of the reaction mechanism.

2.3.2. Oxidation of cytochrome c by tris(oxalato)cobalt(III). Cytochrome c (cyt c) is a relatively small metalloprotein that fluctuates between the ferrous and ferric states. It is an important biological electron-transfer agent. One approach to aid in understanding the *modus operandi* of cytochrome c is to study the kinetics of the intermolecular and intramolecular electron-transfer reactions of redox partners with cytochrome c. A feature of intermolecular reactions is that the kinetic parameters and derived activation parameters obtained can be beset with interpretation difficulties if the properties of the reactants are such that, separation of the contributions from the precursor complex formation equilibrium and the actual electron-transfer rate constant is not possible [148]. This point is illustrated in the reaction scheme given below. One way of countering the difficulty is to use anionic reagents as redox partners for the positively charged cyt c that will generate a sufficiently stable precursor complex. In this regard the tris(oxalato)cobalt(III) trinegative ion, in principle, fits this criterion [149]. The general reaction scheme for oxidation of cyt c^{II} can be outlined as follows equations (14)–(16):

$$[Co^{III}(ox)_3]^{3-} + \text{cyt}c^{II} \rightleftarrows \{[Co^{III}(ox)_3]^{3-} \cdot \text{cyt}c^{II}\} \quad K \tag{14}$$

$$\{[Co^{III}(ox)_3]^{3-} \cdot cytc^{II}\} \rightarrow \{[Co^{II}(ox)_3]^{4-} \cdot cytc^{III}\} \quad k_{ET} \tag{15}$$

$$\{[Co^{II}(ox)_3]^{4-} \cdot cytc^{III}\} \rightarrow [Co(ox)_3]^{4-} + cytc^{III} \quad \text{fast.} \tag{16}$$

The precursor complex formation (equilibrium constant K) is followed by a rate-determining electron-transfer step (rate constant k_{ET}), followed by rapid diffusion apart of the successor complex partners. When the kinetics are carried out in the presence of an excess of Co(III) the rate equation is

$$k_{obs} = \frac{k_{ET}K[Co^{III}]}{1 + K[Co^{III}]}. \tag{17}$$

When ion-pair (precursor complex) formation is very effective, k_{obs} at high [Co(III)] reaches the limiting value k_{ET}. This was shown to be the case for this reaction and thus the activation parameters can be obtained for the actual electron-transfer step for intermolecular electron transfer, not realisable in many other reactions. The value of K was determined to be $253\,dm^3\,mol^{-1}$, $k_{ET} = 0.158\,s^{-1}$ and the second-order rate constant for the overall reaction $(=Kk_{ET}) = 40\,dm^3\,mol^{-1}\,s^{-1}$ at 298 K. Reasonable agreement with these parameters was found from calculations based upon Marcus–Hush theory [143, 144]. An enthalpy of activation value of $73\,kJ\,mol^{-1}$, obtained from measurements in the high [Co(III)] range reflected the slowness of the actual electron-transfer, and the corresponding entropy of activation was close to zero (there is no change in the number of species upon reaching the transition state). Measurement of the volume of activation at high and lower [Co(III)] allowed extraction of the value of ΔV for the ion-pair complex formation. At high [Co(III)], $\Delta V^{\neq} = -5.6\,cm^3\,mol^{-1}$ and at lower [Co(III)], $\Delta V^{\neq} = -11\,cm^3\,mol^{-1}$, meaning that $\Delta V = -5.4\,cm^3\,mol^{-1}$ since $\Delta V^{\neq} = \Delta V(K) + \Delta V^{\neq}(k_{ET})$. Therefore, it was suggested that ion-pair formation between $[Co(ox)_3]^{3-}$ and cyt c^{II} must involve significant overlap of the reactants in terms of their van der Waals radii without significant charge neutralisation, otherwise substantial desolvation would occur. Solvent separation of an ion-pair had been proposed to occur also in the reaction between $[Fe(CN)_6]^{4-}$ and $[Co(NH_3)_5X]^{3+}$ ($X = H_2O$, py, Me_2SO) [150]. The negative volume of activation for electron-transfer within the ion-pair complex can be accounted for by a larger negative contribution caused by increasing electrostriction as the $[Co(ox)_3]^{3-}$ complex ion is reduced to the incipient $[Co(ox)_3]^{4-}$ species, than is the positive contribution arising from the oxidation of cyt c^{II} to cyt c^{III} ($+5\,cm^3\,mol^{-1}$ upon complete oxidation) [151]. An inability to determine kinetic parameters for the reverse reaction or obtain successfully electrochemical data for the overall redox reaction prevented establishment of a volume profile for this system.

2.3.3. The outer-sphere electron transfer between cytochrome c and an anionic Cu(II/I) complex. A goal again was to find a reactant system that binds sufficiently strongly to cytochrome c and thus shows saturation kinetics so that the precursor-formation constant and the electron-transfer rate constant could be separated for both the forward and reverse reactions. Fortunately, the properties of *bis*(ferrozine)copper(II) and the copper(I) analogue were such that this goal was realised; [152] ferrozine is 5,6-*bis* (4-sulphonatophenyl)-3-(2-pyridyl)-1,2,4-triazine (see scheme 8).

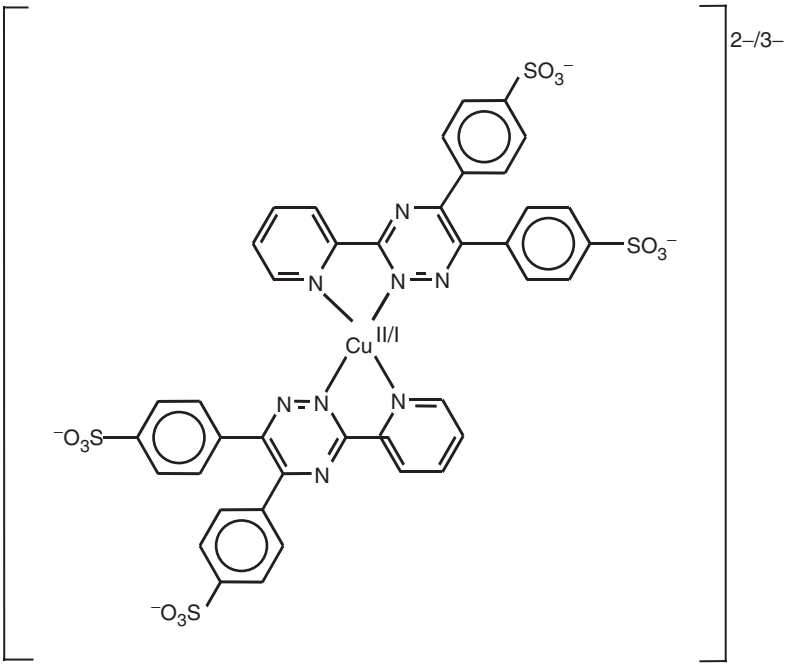

Scheme 8. Copper (II/I) ferrozine complex.

The Cu(II) complex is square pyramidal with a water molecule in a fifth axial position, while the Cu(I) complex is tetrahedral, geometries based primarily on the UV-Vis spectrum. An outer-sphere electron-transfer reaction mechanism is outlined.

$$\mathrm{Cytc^{II}} + [\mathrm{Cu^{II}L_2}]^{2-} \rightleftarrows \{\mathrm{Cytc^{II}}, [\mathrm{Cu^{II}L_2}]^{2-}\} \quad K_{\mathrm{OS}} \tag{18}$$

$$\{\mathrm{Cytc^{II}}, [\mathrm{Cu^{II}L_2}]^{2-}\} \rightarrow \{\mathrm{Cytc^{III}}, [\mathrm{Cu^{I}L_2}]^{3-}\} \quad k_{\mathrm{ET}} \tag{19}$$

$$\{\mathrm{Cytc^{III}}, [\mathrm{Cu^{I}L_2}]^{3-}\} \rightleftarrows \mathrm{Cytc^{III}} + [\mathrm{Cu^{I}L_2}]^{3-} \quad K_{\mathrm{diss}}. \tag{20}$$

The kinetics were monitored over a range of excess Cu(II) concentration and the saturation kinetics obtained at two different ionic strength values could be analysed from the rate law

$$k_{\mathrm{obs}} = \frac{K_{\mathrm{OS}} k_{\mathrm{ET}} [\mathrm{Cu^{II}L_2^{2-}}]}{\{1 + K_{\mathrm{OS}} [\mathrm{Cu^{II}L_2^{2-}}]\}}. \tag{21}$$

A Lineweaver–Burk type reciprocal plot yielded $K_{\mathrm{OS}} = 7.7 \times 10^3\,\mathrm{mol^{-1}\,dm^3}$, and $k_{\mathrm{ET}} = 6.2\,\mathrm{s^{-1}}$ at 15°C and an ionic strength of $0.2\,\mathrm{mol\,dm^{-3}}$. Upon determining the rate constants as a function of temperature at both low and high Cu(II) concentrations, the parameters $\Delta H_{\mathrm{OS}} = -4\,\mathrm{kJ\,mol^{-1}}$, $\Delta H^{\#}_{\mathrm{ET}} = 89\,\mathrm{kJ\,mol^{-1}}$, $\Delta S_{\mathrm{OS}} = +91\,\mathrm{J\,mol^{-1}\,K^{-1}}$ and $\Delta S^{\#}_{\mathrm{ET}} = -79\,\mathrm{J\,mol^{-1}\,K^{-1}}$ were obtained. After considering the charged nature of the reactants and charge distribution on the protein, and local hydrophobic and

hydrophilic phenomena, it was concluded that the enthalpy for outer-sphere complex formation represents a non-specific interaction and the formation is driven by entropy generated in the pre-association process. The electron-transfer step within the outer-sphere complex indicates a significant enthalpic requirement and an entropy change that suggests a structurally constrained process. Rate saturation was exhibited for the reverse process and using an analogous rate law and fitting procedure, values of K_{diss} of $2.0 \times 10^3\,mol^{-1}\,dm^3$ and k_{ET} of $0.014\,s^{-1}$ were obtained. From these data a free energy diagram (see figure 3) for the overall reaction could be generated.

Kinetics measurements at elevated pressures gave rise to ΔV_{OS} of $+0.8\,cm^3\,mol^{-1}$ and $\Delta V_{ET}^{\#}$ of $+8.0\,cm^3\,mol^{-1}$, the small former value being expected on the basis of other measurements and estimates of outer-sphere metal complex pre-associations [150, 153]. In an endeavour to place the transition state on a volume basis for the reaction, the reaction volume was estimated to be $+30\,cm^3\,mol^{-1}$. This is made up of +5, +12 and $+13\,cm^3\,mol^{-1}$ from the contribution from the cyt $c^{II/III}$ couple, the electrostrictive change from the charge change on the Cu centre, and the loss of a water molecule, respectively [142, 151, 153–156]. The axial water molecule is transferred to the bulk water as the coordination number changes from five to four and as the geometry around the copper complex changes from square pyramidal to tetrahedral. The volume

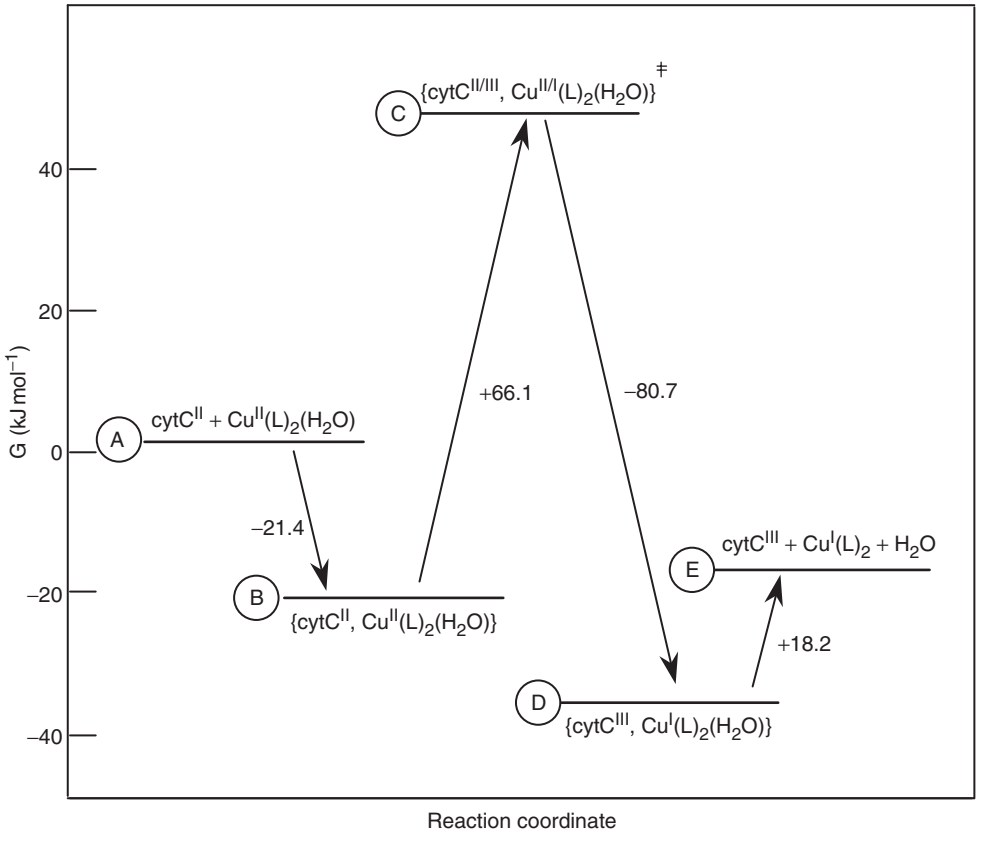

Figure 3. Free energy profile for the overall reaction measured with respect to free energy of the reactants.

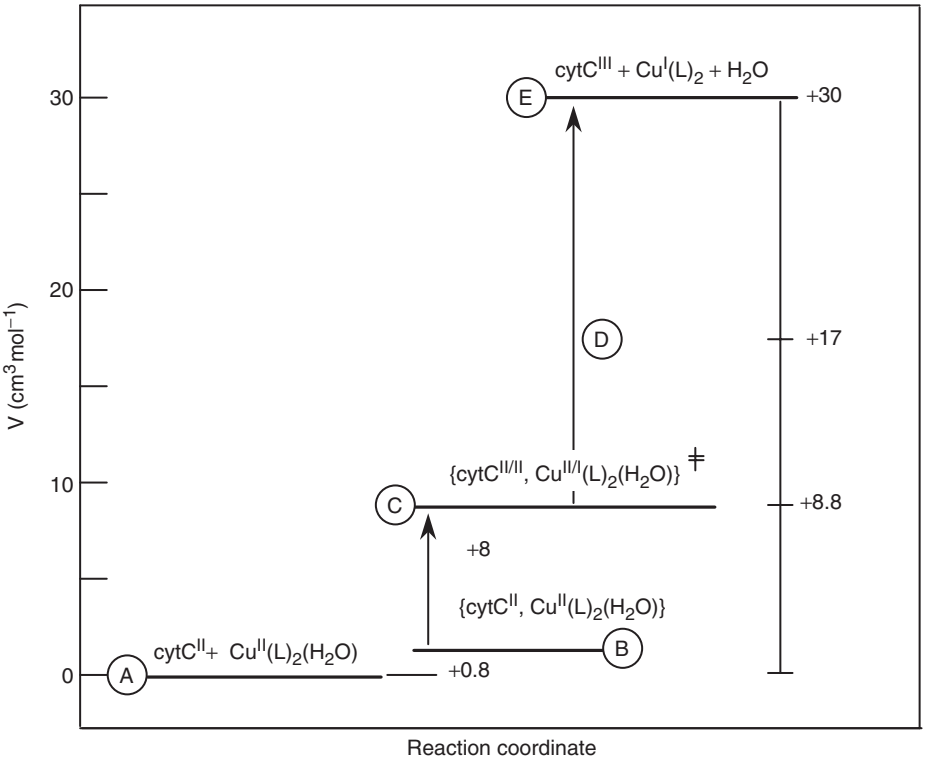

Figure 4. Volume profile for oxidation of cytochrome c by Cu(II)*bis*(ferrozine).

data displayed in figure 4 indicate that the transition state lies early in the overall volume change for the reaction.

This should be compared with redox reactions of cytochrome c with octahedral Ru(III)/Ru(II) complexes where the transition state is at a point very close to 50% of the total volume change [157, 158]. However, in these reactions there is no change in the coordination number. Therefore, in the present system the transition state occurs at a point where the electron is symmetrically poised within the interaction of the cytochrome c with the five-coordinate Cu(II)/(I) species and that the intrinsic volume change due to water loss occurs subsequent to this step.

2.4. *Reactions of NO in coordination chemistry*

It has been demonstrated that nitric oxide (NO) has many important roles in mammalian biology [159–161]. This has resulted in an explosive growth of studies of the interaction of NO with an abundance of other molecules in the last two decades. Of relevance here is the coordination of NO to different metal centres, but particularly of iron. Naturally it is not possible or desirable to cover all the studies pertinent to coordination chemistry, and rather than present a catalogue of reactions, a small number of reports has been selected that have provided some useful insights, but also indicate the challenges, technical and interpretative in this sub-field. The reports that form the basis for sections 2.4.1 and 2.4.2 are certainly not the first time kinetics

measurements of NO reacting with ferro- and ferriheme centres have been made and described [162–165]. However, these newer publications represent additional illumination of the mechanism of interaction of both NO and the nitrite ion with metmyoglobin, and of nitrite ion with methaemoglobin [166, 167].

2.4.1. Mechanistic studies on the reversible binding of nitric oxide to metmyoglobin. Earlier work had addressed the kinetics of what are termed the ''on'' and ''off'' reactions of NO with water-soluble iron(II) and iron(III) porphyrins as simplistic models for ferro- and ferrihaem proteins [168, 169]. Of more interest from a biological perspective is the mechanism of the reaction of NO with metmyoglobin (metMb) itself [166]. The Fe(III) centre is six-coordinate, with a water molecule occupying the position at which NO will coordinate. The spectrum of metMb in the Soret region is modified upon binding of NO and this region represents the most favourable region to exploit for kinetics measurements. Rapid reaction methods (sf and laser flash photolysis) were used to follow the reactions (at pH 7.4) and plots of the pseudo-first-order rate constants *versus* excess [NO] were linear allowing determination of the second-order ''on'' rate constant from the slope and the ''off'' rate constant from the intercept. A temperature- and pressure-dependence study of these kinetics parameters yielded values of $\Delta H^{\#}_{on}$, $\Delta S^{\#}_{on}$ and $\Delta V^{\#}_{on}$ of $65\,kJ\,mol^{-1}$, $+60\,J\,mol^{-1}\,K^{-1}$ and $+20\,cm^3\,mol^{-1}$, respectively. These values were confirmed by a set of parallel experiments employing a laser flash photolysis technique. The large, positive values of the entropy and volume of activation are consistent with the operation of a limiting dissociative mechanism, in which dissociation of the coordinated water molecule must precede formation of the Fe–NO bond. Other evidence indicates that the product MetMb(NO) contains formally a linear Fe^{II}–NO^+ character, signifying that partial charge transfer from NO to Fe^{III} occurs during the bonding process [170, 171]. The value of $\Delta V^{\neq}$ usually associated with dissociation of a coordinated water molecule from an octahedral metal centre is about $+13\,cm^3\,mol^{-1}$ [145]. Therefore it was suggested that some structural rearrangement within the protein may occur during the formation of the five-coordinate metMb in order to account for the value of $+20\,cm^3\,mol^{-1}$.

Activation parameters for the reverse process could not be determined with acceptable precision in some cases from intercepts of k_{obs} *versus* [NO], but a trapping reaction in which excess $[Ru(edta)(H_2O)]^-$ reacts rapidly with NO released from metMb(NO) was devised and employed successfully to obtain the parameters with more reliable values.

$$MetMb(NO) + H_2O \rightarrow metMb(H_2O) + NO \quad k_{off} \tag{22}$$

$$NO + [Ru(edta)(H_2O)]^- \rightarrow [Ru(edta)(NO)]^- + H_2O \quad \text{fast.} \tag{23}$$

The values of $\Delta S^{\#}_{off}$ and $\Delta V^{\#}_{off}$, although the former has a spread of values, are large positive values, and are associated with bond breakage in metMb(NO) and solvational changes associated with solvent reorganisation that occur with charge redistribution and the spin change. The binding step of NO is accompanied by a change from quintet spin state to a diamagnetic complex. The value of $\Delta V^{\neq}$ from stopped-flow experiments is $+16\,cm^3\,mol^{-1}$ and therefore the ''off'' reaction is also of limiting dissociative nature. In turn this means the reaction volume is a small positive value ($5\,cm^3\,mol^{-1}$), that is not surprising, since the overall substitution is of one small neutral molecule

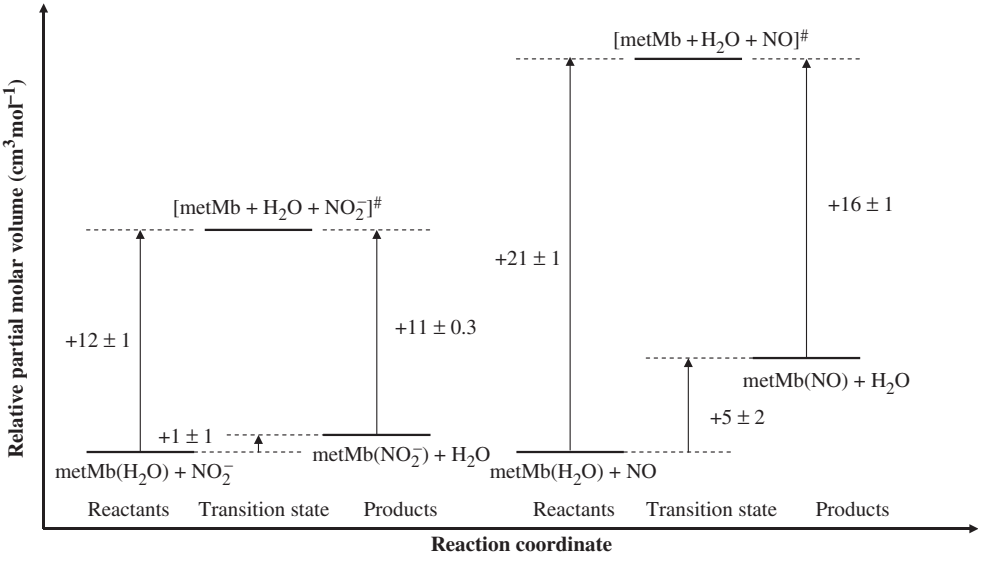

Figure 5. Volume profiles for the reactions (volume given in $cm^3\,mol^{-1}$)

Right: $metMb(H_2O) + NO_2^- \rightleftarrows metMb(NO_2^-) + H_2O$

Left: $metMb(H_2O) + NO \rightleftarrows metMb(NO) + H_2O$.

for another. It was noted that the free radical property of NO does not impart a significant influence on the dynamics of this and other similar reactions, and in fact NO functions more like a typical Lewis base donor. The volume profile is shown below (figure 5) together with that for the corresponding reaction of NO_2^- with metMb.

2.4.2. The mechanism of nitrite ion binding to metmyoglobin and methaemoglobin. Under physiological conditions NO can be metabolised rapidly to nitrite ion or nitrate ion [172]. Establishment of the mechanistic differences or similarities between the binding of NO and nitrite ion to haemoproteins is of chemical and biological interest. There have been kinetic and thermodynamic studies of these reactions but no firm mechanistic conclusions emerged [173]. However, the fact that two anionic ligands, azide and cyanide, have different reactivities toward metMb [174–176], means that a thorough investigation of the kinetics of nitrite binding to metMb and metHb, could prove insightful. One key difference from NO binding to metMb is that spectroscopic observations indicate that nitrite binding to metMb does not lead to a change in the charge on the iron centre. Hence the relevant part of the product is $Fe(III)–NO_2^-$.

The soret region of the visible spectrum could be used for monitoring the kinetics of nitrite binding and under the condition of excess nitrite ion the pseudo-first-order rate constant (k_{obs}) for the reaction,

$$Fe^{III} - H_2O + NO_2^- \rightleftarrows Fe^{III} - NO_2^- + H_2O \qquad (24)$$

can be expressed as:

$$k_{obs} = k_{on}[NO_2^-] + k_{off}. \quad (25)$$

Application of equation (25) generated $k_{on} = 156\,dm^3\,mol^{-1}\,s^{-1}$ and $k_{off} = 2.6\,s^{-1}$ at 20°C at pH 7.4. The former value is more than two orders of magnitude less than that for reaction of NO with metMb ($k_{on} = 2.7 \times 10^4\,dm^3\,mol^{-1}\,s^{-1}$), and the latter is a factor of five lower than the corresponding reaction for NO ($k_{off} = 16\,s^{-1}$) [166]. Therefore, the lower value for the equilibrium constant ($K(NO_2^-)$ *vis a vis* K(NO)) is a consequence mostly of the rate of the binding of NO_2^-. There is a notable decrease in forward and reverse rate constants when the pH is elevated to 8.0, a feature also of reactions of other anionic ligands with metMb. Of the possible reasons for this it was proposed that a change in the total net charge and reorientation of amino acid side chains at different pH values resulting in different electrostatic effects on the reactivity of the iron centre could be a principal contributing factor. The dependence on temperature and on pressure of the forward and reverse reactions of NO_2^- with metMb resulted in the activation parameters, respectively, $\Delta H^{\neq} = 63$ and $109\,kJ\,mol^{-1}$, $\Delta S^{\neq} = +12$ and $+134\,J\,mol^{-1}\,K^{-1}$ and $\Delta V^{\neq} = +12$ and $+11\,cm^3\,mol^{-1}$. These values, with the exception of the entropy of activation in the forward direction, are all consistent with a limiting dissociation mechanism in both directions. Entropy of activation values are often not as reliable as other parameters in mechanistic evaluation. A limiting dissociative mechanism may be written

$$metMb - Fe^{III} - H_2O \rightleftarrows metMb - Fe^{III} + H_2O \quad K_1 = \frac{k_1}{k_{-1}} \quad (26)$$

$$metMb - Fe^{III} + NO_2^- \rightleftarrows metMb - Fe^{III} - NO_2^- \quad k_2, k_{-2} \quad (27)$$

Since k_{obs} is linearly dependent on $[NO_2^-]$, it can be shown readily that $k_{on} = K_1 k_2$ and $k_{off} = k_{-2}$. The reaction volume associated with K_1 should be about $+13\,cm^3\,mol^{-1}$ [156]. It may be inferred that the volume reduction as NO_2^- is bound, and the charge neutralisation effects virtually cancel each other, and the observed value is controlled by the value for the reaction volume relating to K_1. The value of $\Delta V^{\neq}(k_{-2})$ is regarded as typical for bond breakage (volume increase) accompanied by partial charge creation (volume decrease). The volume profiles for reactions of both NO and NO_2^- reacting with metMb are presented in figure 5. The pronounced difference in the value of $\Delta V^{\#}_{(on)}$ can be accounted for by structural changes in the protein as the five-coordinate intermediate is formed (reaction of NO) and changes in electrostriction as the reaction product Fe(II)–NO^+ is formed. The former effect does not appear to be important in the reaction of NO_2^-. The difference in rate constants for the "on" reaction was investigated using DFT calculations and assessment based upon orbital energies provided a compatible explanation.

The ligation of NO_2^- to the four sub-unit methaemoprotein, methaemoglobin (metHb), results in reversible displacement of the coordinated water at the Fe(II) haem centre in each of the four subunits. The kinetics of this process, at pH 7.4, in the presence of excess $[NO_2^-]$, were characterised by a double exponential fit of the absorbance/time data. The association and dissociation rate constants for the fast and slow reactions, as the two stages were described, could be calculated from the plots of pseudo-first-order rate constants *versus* $[NO_2^-]$. Both rate constants for the fast step

were about ten-fold greater than those for the slow step with the faster "on" reaction having about the same rate constant as for reaction of NO_2^- with metMb. In early classic work, Gibson *et al*. have shown that rate constants for the binding of nitrite ion to the isolated ferric α and the β chains, $k_{on}(\alpha)$ and $k_{on}(\beta)$ were 15 and 80 $mol^{-1}\,dm^3\,s^{-1}$ [177]. It is thus reasonable to believe that the fast and slow stages of the present study may be compared with these literature values. The temperature dependence of the kinetics parameters gave rise to distinctly positive enthalpies and entropies for all four reactions, from which it could be concluded that the forward and reverse reactions in both fast and slow stages proceed by a dissociative mechanism. Since it is very likely that pressure could affect the compressibility of the subunits and quaternary structure of metHb, there was not an attempt to determine the dependence on pressure of the kinetic parameters. Consequently the advantage of possession of change in volume properties, valuable in many other contexts, could not be applied in the reaction of metHb with NO_2^-.

2.4.3. Kinetic and mechanistic studies on the reaction of water-soluble iron(III) porphyrin complexes

(a) An octa-anionic Fe(III) porphyrin complex

NO is reactive toward Fe(II) and Fe(III) haem containing systems. This includes iron-porphyrin centres as covered in section 2.4.1. The reactivity of NO toward such centres is governed by the oxidation state of iron and a number of other factors, such as the axial ligands and the type and properties of the substituents on the haem unit of a porphyrin. Several studies of the interaction of nitric oxide with ferrihaem proteins and synthetic Fe(III) porphyrins have been conducted in the interval between the work described here and that in section 2.4.1 [178]. One primary aim is to attempt to establish the influence of the porphyrin microenvironment in a given iron(III) porphyrin, ((P)Fe^{III}), system on the rate and mechanism of NO binding and release and on the stability of the resulting (P)$Fe^{II}(NO)^+$ species toward subsequent reactions in solution. A highly negatively charged water-soluble iron(III) porphyrin, (P^{8-})Fe^{III}, was synthesised and employed in mechanistic studies on its reactivity toward NO [178]. By varying the pH of solution the kinetics results could be obtained for the reversible binding of NO to both (P^{8-})$Fe^{III}(H_2O)_2$ and (P^{8-})Fe^{III}(OH). The octa-anionic complex is shown in scheme 9.

Kinetics measurements of water exchange carried out by ^{17}O NMR spectroscopy indicated a rapid exchange for the diaqua species ($k_{EX} = 7.7 \times 10^6\,s^{-1}$ at 25°C), and strongly suggested a dissociative (I_d or D) pathway for water exchange ($\Delta S^{\neq} = +91\,J\,mol^{-1}\,K^{-1}$ and $\Delta V^{\neq} = +7.4\,cm^3\,mol^{-1}$) [178]. Similar experiments on the monohydroxy species indicated that it probably exists in a five-coordinate form, possibly in equilibrium with a minor fraction of the six-coordinate (P^{8-})Fe^{III}(OH)(H_2O) form. The largest absorbance changes upon adding NO to a solution of (P^{8-})$Fe^{III}(H_2O)_2$ occurred in the Soret region, with less prominent changes at 540 nm. These changes are evidence for the formation of a typical low-spin iron(III) porphinatonitrosyl complex in which the formal charge distribution is shown in the product of equation (28).

$$(P^{8-})Fe^{III}(H_2O)_2 + NO \rightleftarrows (P^{8-})Fe^{II}(NO^+)(H_2O) + H_2O. \qquad (28)$$

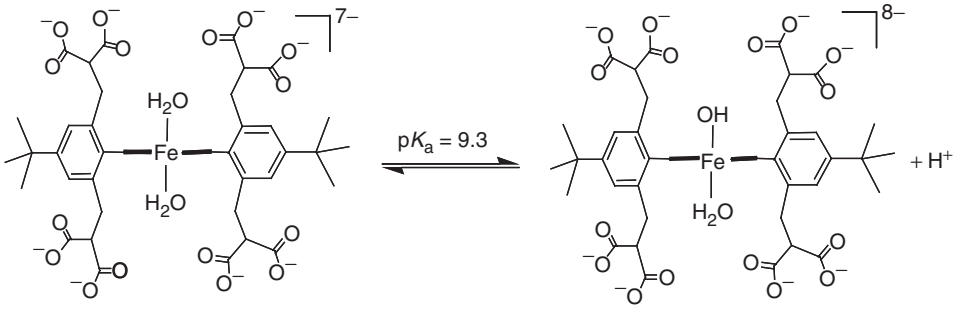

Scheme 9. Proton equilibrium for complex $(P^{8-})Fe^{III}(H_2O)_2$.

A combination of stopped-flow spectrophotometry and a laser flash photolysis method of reaction initiation, followed by visible spectrophotometric monitoring, was used to study the kinetics of the reversible binding of NO to the diaqua complex. This resulted in k_{on} and k_{off} of $8.3 \times 10^3\,mol^{-1}\,dm^3\,s^{-1}$ and $217\,s^{-1}$ respectively, at 24°C, and an equilibrium constant value that agreed reasonably with that determined from equilibrium measurements. Derived values for the activation parameters $\Delta H^{\neq}$, $\Delta S^{\neq}$ and $\Delta V^{\neq}$ are 51 and $105\,kJ\,mol^{-1}$, +40 and $+150\,J\,mol^{-1}\,K^{-1}$, and +6.1 and $+16.8\,cm^3\,mol^{-1}$, for the "on" and "off" reactions, respectively, with the precision of the values of the "off" reaction being improved by application again of the method of using $[Ru(edta)(H_2O)]^-$ as a trapping agent of NO. These values and rate constants could be compared with those acquired for other porphyrin complexes. In general the rate constants for systems with positively charged meso substituents were smaller than those containing negatively charged substituents. However, the activation parameters, particularly $\Delta S^{\neq}$ and $\Delta V^{\neq}$, were quite similar. The volume profile shown in figure 6 for $(P^{8-})Fe^{III}(H_2O)_2$ is therefore a reflection of a common mechanism for NO binding to water-soluble porphyrins, in which rate-determining substitution of an axial water molecule takes place by a dissociative mechanism (I_d or D) followed by volume reduction as a result of spin state change and solvent reorganisation accompanying formation of the low-spin $(P^{8-})Fe^{II}(NO^+)(H_2O)$ product. Important to note is that $\Delta V^{\neq}$ for the "on" reaction is in close agreement with that found for the water exchange process of the diaqua complex, which suggests that the coordination of NO is controlled in rate and mechanism by the water exchange process. The markedly positive $\Delta V^{\neq}$ for the reverse reaction indicates clearly that the release of NO also follows a dissociative mechanism. Breaking the Fe^{II}–NO^+ bond is rate determining and this volume increase is supplemented by that due to formal oxidation (Fe^{II} to Fe^{III}) and spin state change on the iron(III) centre and solvent reorganisation due to neutralisation of the partial charge on the Fe^{II}–NO^+ unit.

Spectroscopic and kinetics studies at a higher pH range, together with speciation analysis, showed that the species reacting with NO at pH 11 is the deprotonated monoaqua species, $(P^{8-})Fe^{III}(OH)$. In contrast to the results for some other aqua-metal complexes [179], the hydroxo form here is less reactive than the diaqua form in reaction with NO ($k_{on} = 5.1 \times 10^4$ *versus* $8.2 \times 10^5\,mol^{-1}\,dm^3\,s^{-1}$ at 25°C). This reduction can be explained in conjunction with the interpretation of the activation parameters cited below; the formation of $(P^{8-})Fe^{II}(NO^+)(OH)$ from the five-coordinate hydroxo form is not controlled by the lability of the Fe^{III} centre but rather by the enthalpy and entropy

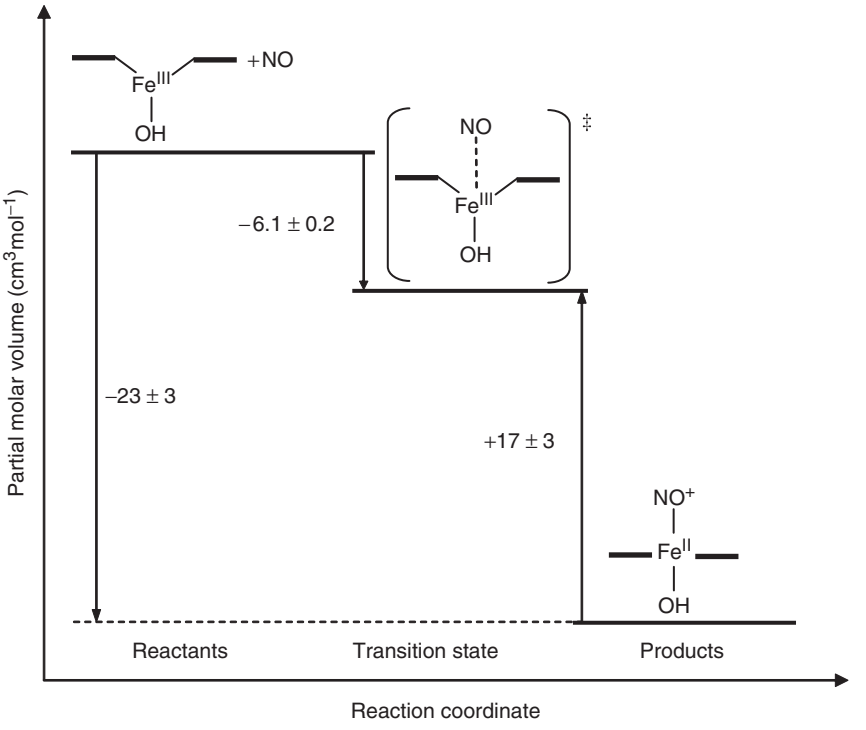

Figure 6. Volume profile for the reversible binding of nitric oxide to $(P^{8-})Fe^{III}(OH)$.

changes associated with spin reorganisation and structural rearrangements upon formation of the Fe^{II}–NO^+ bond. For the "on" reaction $\Delta H^{\neq} = 34.6\,kJ\,mol^{-1}$, $\Delta S^{\neq} = -39\,J\,mol^{-1}\,K^{-1}$ and $\Delta V^{\neq} = -6.1\,cm^3\,mol^{-1}$, indicating a changeover from NO binding dissociatively to the diaqua complex, to associatively binding to the hydroxo species. In analogy with the reversible binding of NO to the high-spin five-coordinate $(P)Fe^{III}(Cys)$ centre in substrate bound Cytochrome $P450_{cam}$, [180] the reaction of the hydroxo species with NO first proceeds in a diffusion-controlled step to an encounter complex, followed by an associatively activation-controlled mechanism with an "early" transition state and spin reorganisation occurring at the Fe^{III} centre controlling the rate to a large extent. The scheme (scheme 10) shows that in the product Fe^{II} is coplanar with the porphyrin unit.

The volume of activation for the reverse reaction is $+17\,cm^3\,mol^{-1}$, a value that represents volume expansion caused by partial Fe^{II}–NO^+ bond cleavage and $S = 0$ to $S = 5/2$ spin change, and solvent expansion. The volume change properties are displayed in figure 6.

(b) The mechanism of the reversible binding of NO to a water-soluble octa-cationic Fe^{III} porphyrin complex.

The complex shown, $(P^{8+})Fe^{III}(L)_2$, $L = H_2O$ or OH^-, (scheme 11) synthesised earlier was initially investigated to determine the species present over a range of pH and to obtain the rates of water exchange, and to compare and contrast these properties with those for the octa-anionic complex of section 2.4.3(a) [181].

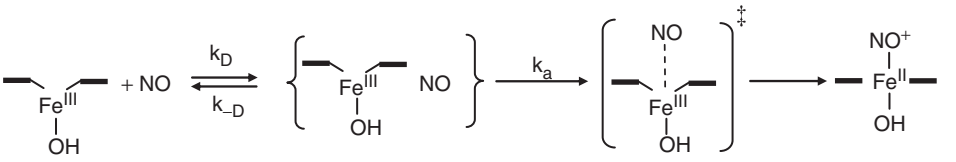

Scheme 10. Reaction sequence for $(P^{8-})Fe^{III} + NO$.

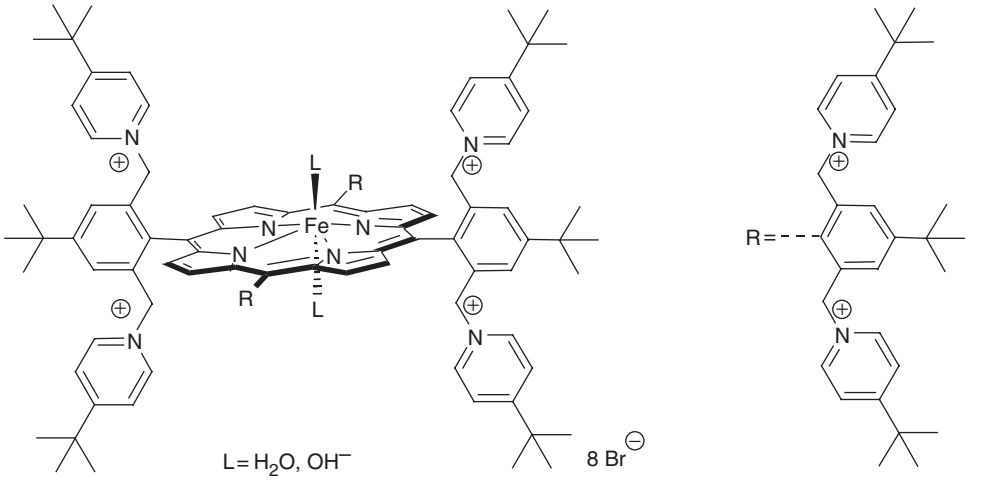

Scheme 11. Structure of $(P^{8+})Fe^{III}(L)_2$.

For the diaqua complex $k_{EX} = 5.5 \times 10^4\,s^{-1}$, and for the monohydroxo-ligated $(P^{8+})Fe^{III}(OH)(H_2O)$, $k_{EX} = 2.4 \times 10^6\,s^{-1}$, at 25°C, the former of which is the smallest value of k_{EX} reported for $(P)Fe(H_2O)_2$ porphyrins. Thus the lability of the metal centre is decreased by the influence of the positively charged meso substituents on the porphyrin periphery, which therefore, apparently stabilise the Fe^{III}–H_2O bond through inductive electronic effects. The acceleration of water exchange on the hydroxo-species is consistent with a *trans*-labilising effect of the OH^- ligand. Note that the hydroxo-species here differs from the octa-anionic species in that it is not principally five-coordinate. Compared with other porphyrin complexes for which comparison can be made, the volumes of activation for water exchange are much less positive ($\Delta V^{\neq} = +1.5$ and $+1.1\,cm^3\,mol^{-1}$ for the diaqua and monohydroxo species respectively), and these values are those that permitted a pure interchange mechanism to be proposed.

Reaction of $(P^{8+})Fe^{III}(H_2O)_2$ with NO is rapid, generating $(P^{8+})Fe^{II}(NO^+)(H_2O)$, and this is followed by a second slower reaction that was not characterised or analysed in this report.

$$(P^{8+})Fe^{III}(H_2O)_2 + NO \rightleftarrows (P^{8+})Fe^{II}(NO^+)(H_2O) + H_2O \tag{29}$$

$$(P^{8+})Fe^{II}(NO^+)(H_2O) + NO \rightleftarrows (P^{8+})Fe^{II}(NO) + NO_2^- + 2H^+. \tag{30}$$

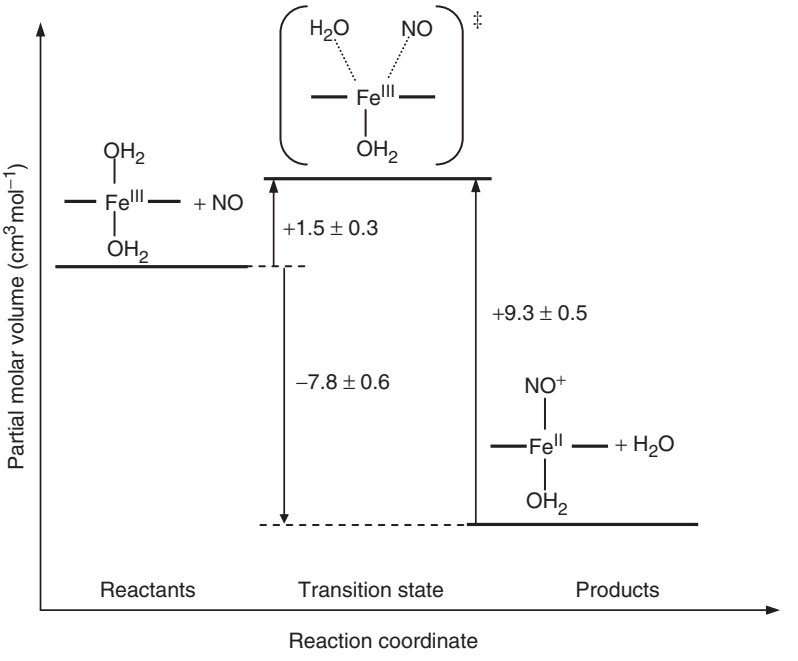

Figure 7. Volume profile for the reversible binding of nitric oxide to $(P^{8+})Fe(H_2O)_2$.

The forward and reverse rate constants reflected slower reactions than for other related porphyrins and indicate that the positively charged meso groups stabilise both the Fe–H_2O and Fe^{II}–NO^+ bonds. An analysis of kinetic parameters for this and other porphyrins binding to NO showed that the influence of steric or electrostatic effects is not necessarily minor. The main factor tuning the dynamics of binding to diaqua species is the modulation of electron density on the iron centre by the porphyrin macrocycle. The volume profile based on values of $\Delta V^{\#}_{on}$ and $\Delta V^{\#}_{off}$ of +1.5 and +9.3 $cm^3\,mol^{-1}$ respectively may be interpreted as an I mechanism for the "on" reaction as the Fe–H_2O bond is markedly stabilised, as noted above. The "off" reaction volume of activation is less than that for other porphyrins, implying a less dissociative mode for NO release. See volume profile in figure 7.

The reactivity of $(P^{8+})Fe(OH)(H_2O)$ toward NO is characterised by a decrease in k_{on} relative to that of the diaqua species, a feature shared by the k_{off} value, and in common with corresponding properties of other porphyrins. The water exchange rate is faster than it is for the diaqua species; consequently the decrease in the rate of NO binding is not controlled by the lability of the metal centre but by electronic and structural changes. These mainly involve the reorganisation of spin density at the Fe(III) centre. The volume profile for this reaction demonstrates again the associative nature of the binding of NO ($\Delta V^{\#}_{on} = -13.8\,cm^3\,mol^{-1}$), but points to a "later" transition state than operates for comparable reactions of porphyrin complexes with NO. The reaction volume of $-16.4\,cm^3\,mol^{-1}$ is smaller than for related reactions, a difference ascribed to the presence of a weakly bound water molecule in $(P^{8+})Fe(OH)(H_2O)$ that is released upon coordination of NO, partially compensating the volume decrease associated with the formation of the Fe^{II}–NO^+ bond. Such a partial compensation cannot occur for the five-coordinate hydroxo-porphyrins. See volume profile in figure 8.

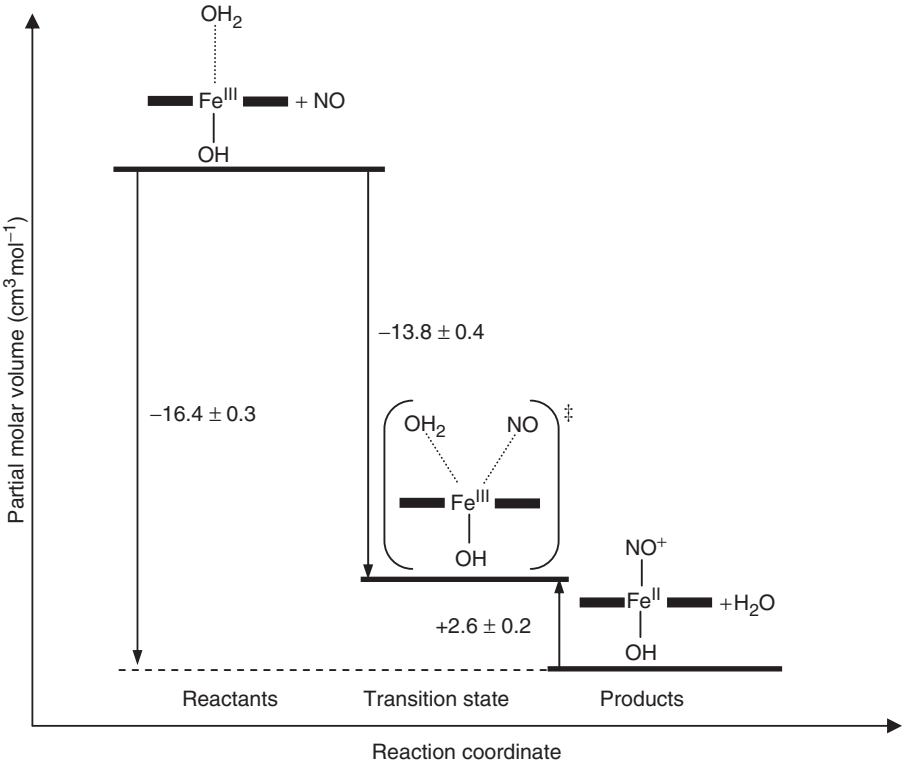

Figure 8. Volume profile for the reversible binding of nitric oxide to $(P^{8+})Fe(OH)(H_2O)$.

This report contains a perspective of the reasons for the similarities and differences in kinetic properties and mechanism for the octa-cationic and other porphyrins.

A range of other investigations of the kinetics of interaction of NO with transition metal centres has been reported. These include the reversible binding of NO to Fe(II) aminocarboxylate and related complexes [182, 183], substituent influence on the reductive nitrosylation of Fe(III)-porphyrins and the catalytic role of the nitrite ion [184], the influence of terpyridine on the kinetics and mechanism of the reaction of NO with *cis* and *trans* Ru(III)-terpy complexes [185], mechanistic studies on the binding of NO to a synthetic haem-thiolate complex relevant to cytochrome P450 [186], NO binding to cytochrome $P450_{cam}$ which is enhanced by substrate binding [180], a further analysis of the mechanism of nitrosylation of water-soluble Fe(III)-porphyrin complexes [187] and a mechanistic analysis of the reductive nitrosylation of water-soluble Co(III)-porphyrins [188]. In a slightly different vein a report on the structure and characterisation of non-cyclic tetraaza complexes of Cu(II) and their reactions with nitric oxide has appeared [189].

2.5. *Other reactions*

2.5.1. Transition state characterisation for reversible binding of dihydrogen to $(bpy)_2$rhodium(I). The nature of the interaction of dihydrogen with low-valent metal

centres and the formation of molecular dihydrogen complexes or high–valent dihydrogen complexes are subjects of considerable interest [190]. In a relatively early paper the oxidative addition of H_2 to $Rh^{I}(bpy)_2^+$ to form the *cis*-dihydride-rhodium(III) complex was investigated [191].

$$Rh^{I}(bpy)_2^+ + H_2 \rightleftarrows cis\text{-}Rh^{III}(H)_2(bpy)_2^+ \quad k_f, k_r. \tag{31}$$

Both rate constants could be determined ($k_f = 24.4\,mol^{-1}\,dm^3\,s^{-1}$ and $k_r = 1.70 \times 10^{-2}\,s^{-1}$ in acetone, at 25°C) and their combination yielded the same value for the equilibrium constant as was obtained from equilibrium measurements ($K_H = 1.45 \times 10^3\,mol^{-1}\,dm^3$). A further study aimed at providing more insight into the nature of the transition state has been published recently [192]. Water was avoided as a solvent again in order to remove the possibility of a multiplicity of initial Rh(I) species. The reaction was monitored in both methanol and acetone and also as a function of temperature and pressure. Kinetic and activation parameters and parameters relating to the equilibrium differed little between the two solvents. For the forward reaction the activation enthalpies were about $40\,kJ\,mol^{-1}$ and the activation entropies were in the range -75 to $-95\,J\,mol^{-1}\,K^{-1}$, the latter being consistent with an associative reaction, a consistency supported by the reaction entropies ($-80\,J\,mol^{-1}\,K^{-1}$). The investigation produced a conundrum in that the reaction volumes, and activation volumes in the forward direction, were essentially identical, (*ca* $-15\,cm^3\,mol^{-1}$) meaning there was no volume change upon reaching the transition state in the reverse direction. The value of $\Delta V^{\neq}$ in the forward direction was less than anticipated based upon comparable oxidative addition reactions [193–195]. It was suggested that bulky bipyridine ligands dominate the partial molar volumes of the Rh complexes, while dihydrogen and dihydride are comparatively small ligands. It was proposed that the transition state includes the dihydrogen within the coordination sphere of the Rh complex and would possess a volume that is insensitive to the actual Rh–H or H–H distances. These and other arguments, including calculations (B3LYP hybrid Density Functional Theory), supported these explanations and the very late transition state in the forward direction. The kinetic and equilibrium parameters for both solvents are illustrated in enthalpy, entropy and partial molar volume profiles (figure 9).

2.5.2. The kinetics of dissociation of tris(diimine)iron(II) complexes. Diimine ligands such as phen and bpy have been widely used as sensitive spectrophotometric reagents for estimation of Fe(II). The limited solubility in aqueous media has been overcome by preparing sulphonated derivatives, the 3- and 5-sulphonic acid derivatives of phen, for example Other ligands that have been synthesised, ferene (fer = {3-(2-pyridyl)-5,6-*bis*(5-furyl sulphonic acid)}) [196, 197], ferrozine (fz or ppsa = {3-(2-pyridyl)-5,6-*bis*(4-phenyl sulphonic acid)-1,2,4-triazine)}) [198, 199], yield tris complexes with Fe(II), possessing molar extinction coefficients in the range of $30{,}000\,dm^3\,mol^{-1}\,cm^{-1}$, almost three times the value for the equivalent phen complexes, thus extending the chromophoric power of these reagents for iron(II) (see scheme 12).

Analysis of Fe(II) in various aqueous media applications drove this development. In other applications lipohilic, non-sulphonated diimines may be required. One example is the unsulphonated ferene, fertri. In order to apply these ligands reliably, analytically the properties of stability and lability of the tris-iron(II) complex in different media need to be established. These features of the $[Fe(fer)_3]^{4-}$ complex were determined much

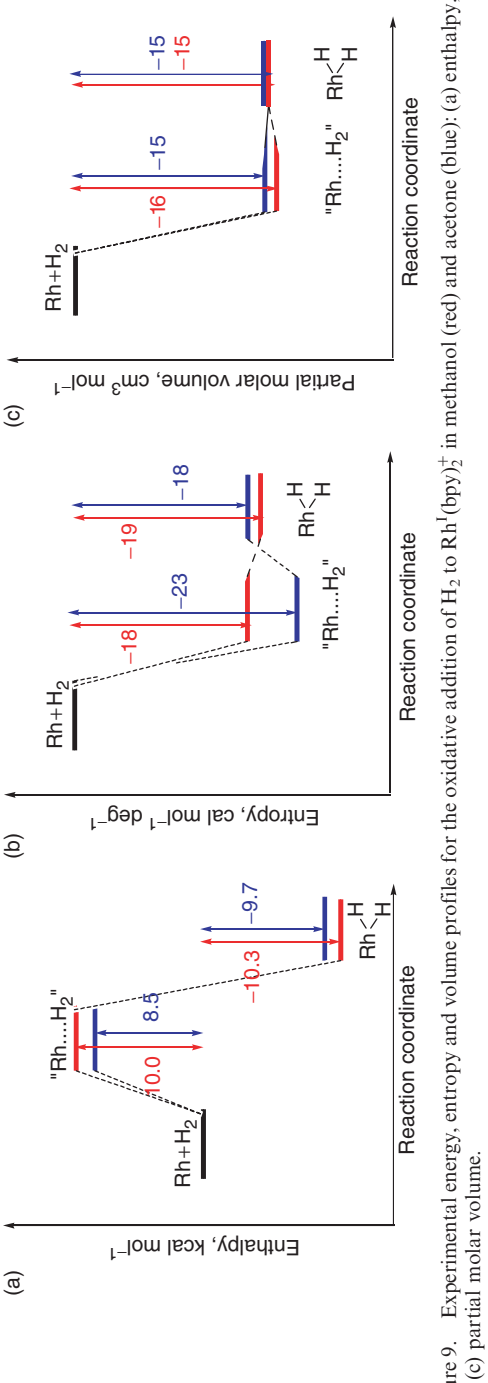

Figure 9. Experimental energy, entropy and volume profiles for the oxidative addition of H_2 to $Rh^{I}(bpy)_2^+$ in methanol (red) and acetone (blue): (a) enthalpy, (b) entropy and (c) partial molar volume.

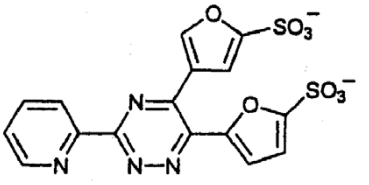

Scheme 12. Bidentate ligands: ferene and ferene triazine.

earlier and the principal noteworthy characteristic was that base hydrolysis occurred in two detectable stages, one in the sf range and a second in a conventional time range [200]. In most cases (tris)diimine complexes of Fe(II) dissociate with a single rate-determining step (pseudo-first order in the presence of excess of $[OH^-]$). In two-step base hydrolysis it has been proposed that initially a ligand molecule is modified by ligand hydroxylation and subsequently the ligands are detached from the metal centre [201, 202]. In a more recent study [203] the base hydrolysis of $[Fe(fertri)_3]^{2+}$ in 25 or 40% aqueous methanol was also found to occur in two steps, the former of which may be represented:

$$[Fe(fertri)_3]^{2+} + OH^- \rightleftarrows [Fe(fertri)_2(fertriOH)]^+. \quad (32)$$

The kinetic results for the second stage are consistent with rate laws established for base hydrolysis of tris(diimine) Fe(II) complexes; [7, 204] *viz*.

$$\frac{d[FeL_3^{2+}]}{dt} = \{k_1 + k_2[OH^-] + k_3[OH^-]^2\}[FeL_3^{2+}], \quad (33)$$

where L = diimine ligand.

k_1 is small and represents rate limiting dissociation, or in this case the reverse reaction of equation (32). The k_3 term manifests itself only at higher $[OH^-]$. Because the second step involves hydroxide ion reacting with an equilibrium mixture of the tris complex and the hydroxylated *bis* complex interpretation of the term k_2 is complicated. While base hydrolysis is a mechanistically challenging process to understand, scavenging by an excess of a competing ligand followed a simple dissociation (for example, $k = 3.1 \times 10^{-5}\,s^{-1}$ in 50% methanol at 30°C, using a large excess of phen in a solution of $[Fe(fertri)_3]^{2+}$). Dissociation in HCl solution was faster indicating that it is not only a reaction of scavenging a ligand donor atom, but some H^+ catalysis, either through ligand protonation in the starting complex or in an intermediate, occurs. It can be concluded that in a neutral environment both $[Fe(fer)_3]^{4-}$ and $[Fe(fertri)_3]^{2+}$ form a complementary pair of substitution-inert complexes for the spectrophotometric determination of iron, but the mechanism of base hydrolysis remains unclear.

2.5.3. Dynamics of fluxional motion in platinum phenanthroline complexes containing phosphorus donor atoms. The fluxional motion of 2,9-dimethyl-1,10-phenanthroline (dmphen) between non-equivalent exchanging sites in cationic complexes of the type $[Pt(Me)(dmphen)(L)]^+$, where L is a neutral donor ligand, has been characterised [205–207]. The mechanism can switch between associative and dissociative pathways.

Upon varying the solvent, the counter-ion, and the electronic and steric characteristics of L, the rate and mechanism of the dynamic exchange of the coordinated dmphen ligand can be altered and thus amenable to fine-tuning. Upon adding more steric bulk (through ortho-methoxyphenyl groups) to the phosphorus donor atom, the fluxional motion in $[Pt(Me)(dmphen)(PR_3)]^+$ is decreased with increasing steric congestion at PR_3 [208]. These motions that showed that the rates of flipping for tris(2-methoxyphenyl)phosphane and the *bis* analogue were identical with that for dmphen, were obtained from NMR spectroscopic measurements. For example, the rate constants for the rates of N–N flipping at 340 K in $CDCl_3$, are $579 \times 10^3\,s^{-1}$, $195 \times 10^3\,s^{-1}$ and $21.8 \times 10^3\,s^{-1}$ for $[Pt(Me)(dmphen)(P(2\text{-}MeOC_6H_4)Ph_2)]^+$, $[Pt(Me)(dmphen)(P(2\text{-}MeOC_6H_4)_2Ph)]^+$ and $[Pt(Me)(dmphen)(P(2\text{-}MeOC_6H_4)_3]^+$, respectively. The rate constant for phosphane rotation in the last of those compounds was also $21.8 \times 10^3\,s^{-1}$. Rationalisation of these results was presented by a combination of arguments that could be deduced from ORTEP diagrams and the possibility of three coordinate intermediates, five-coordinate intermediates (a Berry pseudo-rotation or a turnstile mechanism), rates of ring opening or closure. All hypotheses were supported with detailed schemes. The outcome was the design of molecules whose properties could be fine-tuned, based on the analysis of other results and those cited.

2.6. *Computational aspects*

Theoretical calculations that are in direct support of experimental results have been reported in sections 2.1.3, 2.2.4.1 and 2.5.1. In addition there have been many reports dedicated to calculations particularly of the more simple process of water exchange on fully aquated metal ions or those aqua-ions also containing spectator ligands, particularly of transition metal ions and lanthanide ions as indicated above. Other computational studies have focused upon the water exchange between the first and second coordination spheres. An impressively lucid account of this area of study has been provided [209]. It contains details of the assumptions, limitations and representative examples of application of techniques such as molecular orbital theory, density functional theory, continuum models and molecular dynamics methods, and should be consulted for coverage of the topic up to the beginning of 2003. In this article by way of example three recent theoretical studies are presented.

2.6.1. Nitric oxide binding to cobalamin: influence of the metal oxidation state. This theoretical study [210] is part of a wider analysis of the redox-controlled binding of NO by transition metal complexes [211]. Model systems for cobalamin, shown (scheme 13), were chosen for calculation purposes.

The underlying theme of this study is to determine why cob(II)alamin can bind NO in aqueous solution and cob(III)alamin does not. The Co(II) oxidation state form was found to bind water more strongly than NO in the gas phase; however, when solvation effects are included *via* the polarisable continuum model, NO binding is more favourable. Hence the explanation that NO is observed experimentally to bind to cob(II)alamin in aqueous solution is that this is a result of a weak complexation by the cobalt(II) species of water and the relatively poor solvation of NO. Calculated vibrational frequencies support an interpretation of the cob(II)alamin-NO complex as being in effect cob(III)alamin-NO^-. Hartree–Fock calculations are consistent with the

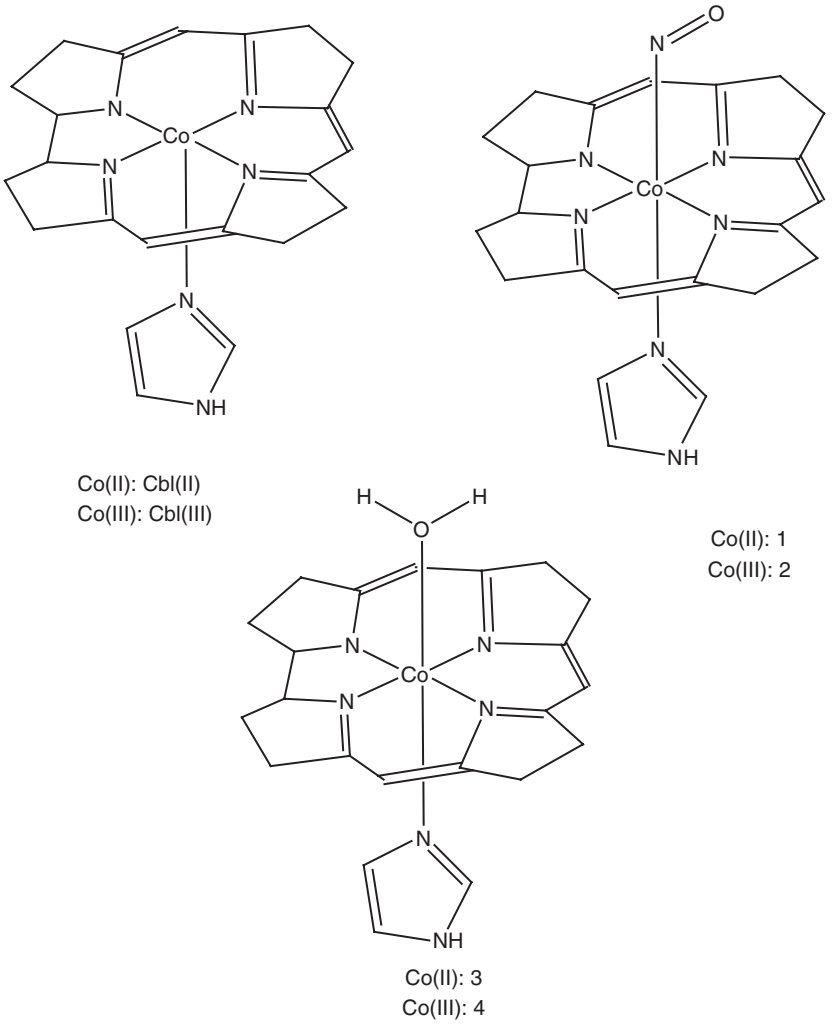

Scheme 13. Different cobalamin complexes studied.

degree of charge transfer although DFT calculations underestimate the degree of charge transfer.

2.6.2. Ligand exchange processes on solvated beryllium cations. Experimentalists had studied solvent exchange on Be^{2+} ions, and determined volumes of activation that ranged from distinctly negative in value ($-13.6\,cm^3\,mol^{-1}$ for water) and indicative of a limiting A-mechanism, to distinctly positive in value ($+10.5\,cm^3\,mol^{-1}$ for tmu (tmu = N,N,N,N-tetramethylurea)) and indicative of a limiting D-mechanism [212]. Intermediate values, more indicative of interchange character were, for example, $-2.5\,cm^3\,mol^{-1}$ for dmso, $-4.1\,cm^3\,mol^{-1}$ for trimethylphosphate, $-3.1\,cm^3\,mol^{-1}$ for

dimethylformamide (I_a), and $+10.3\,cm^3\,mol^{-1}$ for N,N-dimethylpropyleneurea (I_d). The basis for the assignment was made partly upon the limiting values of -13 or $+13\,cm^3\,mol^{-1}$ for A and D mechanisms, respectively, for water exchange from octahedral complexes [156]. Since solvated Be^{2+} ions are tetrahedrally coordinated this implied guideline may not be wholly appropriate. In order to illuminate further the mechanism of ligand exchange upon Be^{2+} ions, the dynamics of the coordination chemistry were investigated by high-level DFT and *ab initio* computations [213]. The emphasis was on H_2O and NH_3, but model solvents such as molecular nitrogen, hydrogen cyanide, carbon monoxide, carbon dioxide and formaldehyde were also assessed. The method involved optimising structures at a version of the Lee–Yang–Parr function, and these were characterised as minima or transition state structures by computation of vibrational frequencies. For the ligands in question the calculations showed that an I_a mechanism was followed and the magnitude of the activation barrier was almost independent of the donor atom. Yet differences in the activation barrier related more to the hybridization undergone by the ligand donor atom. This means that steric effects can play a major role in solvent exchange in Be^{2+} systems. Thus the sterically crowded molecules in the experimental study favour a three coordinate transition state whereas for the small ligands, with insignificant steric factors (in the context of the process), the transition state is likely to resemble a five-coordinate trigonal bipyramid.

2.6.3. Ligand exchange processes on solvated lithium cations. Compounds of lithium are used extensively in synthesis, industrial applications and medicine. Fundamental knowledge of basic processes such as solvent exchange on solvated lithium(I) cations can be a useful prerequisite to understanding complex reactions. The expectation that solvent exchange on Li^+ would be extremely rapid (k_{EX} ca $10^9\,s^{-1}$ for water exchange) was confirmed by the lack of detection of line broadening in NMR spectroscopic signals employing ^{17}O in aqueous solutions of Li^+. Thus resort was made to theoretical methods to attempt to understand water and other solvent exchange processes. A method involving a cubic simulation box containing 512 water molecules and one lithium cation gave rise to the proposition that water exchange occurred through an associative or an associative interchange mechanism [214], but this study did not contain detail of the transition states for these mechanisms.

The first coordination shell around Li^+ in aqueous solution consists of four tightly bound water molecules. Additional water molecules do not coordinate to the lithium cation, but rather form a second coordination sphere with hydrogen bonds to the coordinated water molecules. Calculations using DFT methods indicate that water exchange proceeds through a trigonal bipyramidal reactive intermediate $[Li(H_2O)_5]^+$ that is reached via a late transition state [215]. The entering water molecule approaches the lithium cation in a direct manner and has the effect of pushing two coordinated water molecules toward axial positions. An energy profile of the exchange could be developed. Computed molecular volumes showed that the intermediate is more compact than the precursor complex, $[Li(H_2O)_4(H_2O)]^+$, clearly indicating a limiting associative mechanism. The molecular dynamics simulations predicted that the entering water molecule approaches the tetrahedral $[Li(H_2O)_4]^+$ species through a face of the tetrahedron and the reaction proceeds with an S_N2-like *trans* exchange stereochemistry. The mechanism derived from the DFT study was one in which the entering molecule

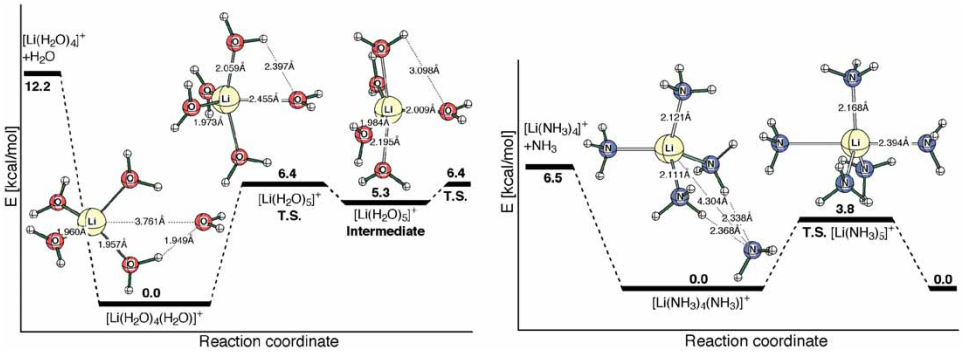

Figure 10. Energy profile for water exchange (left) and ammonia exchange (right) around the lithium cation (relative energies: B3LYP/6-311 + G**).

assumes an equatorial position and the reaction proceeds with *cis* stereochemistry. The latter mechanism is strongly supported by energy calculations and by arguments based upon the high fluxionality of $[Li(H_2O)_5]^+$.

The DFT method was also employed to analyse the exchange of NH_3 on $[Li(NH_3)_4]^+$ [215]. The interaction of an ammonia molecule with $[Li(NH_3)_4]^+$ is weaker than the corresponding interaction in the aqueous based system, and illustrates an unexpected feature, in that the structure of $[Li(NH_3)_4(NH_3)]^+$ shows the fifth ammonia molecule forming two long, weak bonds to two different NH_3 ligands in the first coordination sphere. The expectation would be that only one H–bond would form as ammonia has only one lone pair. Ammonia exchanges with *trans* stereochemistry in a similar fashion to an S_N2 mechanism. The entering and leaving ammonia molecules are axial in the five-coordinate transition structure and possess rather long N to Li bonds, whereas the three in-plane NH_3 ligands show modestly lengthened Li–N bonds. The specifics of the computed bond lengths are typical for an associative interchange mechanism. The influence of the bulk solvent was negligible, as was the case of exchange of water. It was conjectured that NH_3 may exchange faster than water. The difference in mechanism between water exchange and ammonia exchange on Li^+ was attributed to the nature of the Li–O *versus* the Li–N bonds. In water the fifth ligand is relatively strongly bound, whereas in ammonia the fifth ligand is bound to Li^+ more weakly. The energetic order for other bound ligands was consistent with qualitative expectations based on sizes and electronegativities. The conclusion overall is that the mechanism of water exchange around the lithium cation can be thought of as borderline between associative and associative interchange, and the mechanism of ammonia exchange around the cation is associative interchange. The transition states for both water exchange and ammonia exchange on a lithium cation are shown in figure 10.

3. Concluding comments

The results and conclusions from a selection of mechanistic studies of reactions of coordination complexes, mostly from recent reports, have been described. Reactions

that have been initiated photochemically (except in conjunction with normal thermal methods) or by pulse radiolysis methods and reactions studied electrochemically have not been included. Nevertheless, the studies cited represent a wide range of fascinating and interesting chemistry, and should stimulate and encourage those engaged in this field of endeavour and indeed induce others to participate in these areas of research. Further details and a wider background may be gleaned from the individual reports and reviews, respectively, cited in the bibliographic section.

Acknowledgements

The authors gratefully acknowledge the dedication of their colleagues, coworkers and collaborators who have participated in the research projects reported in this article. Naturally the contributions reported herein from other groups in the wider coordination chemistry mechanisms community are also acknowledged. Financial support for our work came from the Deutsche Forschungsgemeinschaft, Fonds der Chemischen Industrie, Alexander von Humboldt Foundation and DAAD.

References

[1] D.D. Brown, C.K. Ingold, R.S. Nyholm. *J. Chem. Soc*., 2674 (1953).
[2] C.K. Ingold, R.S. Nyholm, M.L. Tobe. *J. Chem. Soc*., 1691 (1956).
[3] C.K. Ingold, R.S. Nyholm, M.L. Tobe. *Nature*, **194**, 344 (1962).
[4] T.S. Lee, I.M. Kolthoff, D.L. Leussing. *J. Am. Chem. Soc*., **70**, 3596 (1948).
[5] H. Taube. *Chem. Rev*., **50**, 69 (1952).
[6] F. Basolo, R.G. Pearson. *Mechanisms of Inorganic Reactions*, Wiley, New York (1958, 1967).
[7] D.W. Margerum. *J. Am. Chem. Soc*., **79**, 2728 (1957).
[8] D.R. Stranks, R.G. Wilkins. *Chem. Rev*., **57**, 741 (1957).
[9] T. Moeller. *Inorganic Chemistry*, Wiley, New York (1952).
[10] E.de.B. Barnett, C.L. Wilson. *Inorganic Chemistry*, Longmans, Green and Co., London (1953).
[11] H.J. Emeléus, J.S. Anderson. *Modern Aspects of Inorganic Chemistry*, 2nd Edn, Routledge and Kagan Paul, London (1952).
[12] T.J. Swift, R.E. Connick. *J. Chem. Phys*., **37**, 307 (1962).
[13] Q.H. Gibson, L. Milnes. *Biochem. J*., **91**, 161 (1964).
[14] M. Eigen, L. de Maeyer. In *Investigation of Rates and Mechanisms of Reactions*, S.L. Friess, E.S. Lewis, A. Weissberger (Eds), Part II, Chapter 18, Interscience, New York (1963).
[15] E.F. Caldin. *Fast Reactions in Solution*, Blackwell, Oxford (1964).
[16] H. Hartridge, F.J.W. Roughton. *Proc. Roy. Soc*., **104**, 376, London (1923) London.
[17] B. Chance. *J. Franklin Inst*. 229, 455, 613, 737, (1940).
[18] Q.H. Gibson. *Disc. Faraday Soc*., **17**, 137 (1954).
[19] Q.H. Gibson, F.J.W. Roughton. *Proc. Roy. Soc. B*, **143**, 310 (1955).
[20] G. Czerlinski, M. Eigen. *Z. Elektrochem*., **63**, 652 (1959).
[21] A.K.S. Ahmed, R.G. Wilkins. *J. Chem. Soc*., 2901 (1960).
[22] A.G. Davies, W.MacF. Smith. *Proc. Chem. Soc*., 380 (1961).
[23] G.G. Hammes, J.I. Steinfeld. *J. Am. Chem. Soc*., **84**, 4639 (1962).
[24] C.H. Langford, H.B. Gray. *Ligand Substitution Processes*, Benjamin, New York (1965).
[25] Specialist Periodical Reports, *Inorganic Reaction Mechanisms*, Vol. 1, 1971; Vol. 2, 1972; Vol. 3, 1974; Vol. 4, 1976; Vol. 5, 1976; Vol. 6, 1979; Vol. 7, 1981; Volumes 1–3, Senior Reporter, J. Burgess; Volumes 4–6, Senior Reporter, A. McAuley; Volume 7, Senior Reporter, G. Sykes. Volumes 1–6 published by The Chemical Society, Volume 7 published by the Royal Society of Chemistry.
[26] J. Burgess. *Metal Ions in Solution*, Ellis Horwood, Chichester, Chapters 11–14 and references *loc cit*, 1978.

[27] M.V. Twigg (Ed.). *Mechanisms of Inorganic and Organometallic Reactions*, Vols. I–VII. Plenum, New York (1983–1994).
[28] R.G. Wilkins. *Kinetics and Mechanism of Transition Metal Complexes*, VCH, Weinheim (1991).
[29] J.H. Espenson. *Chemical Kinetics and Reaction Mechanisms*, 2nd Edn, McGraw-Hill, New York (1996).
[30] R.B. Jordan. *Mechanisms of Inorganic and Organometallic Systems*, 2nd Edn, Oxford University Press, Oxford (1998).
[31] M.L. Tobe, J. Burgess. *Inorganic Reaction Mechanisms*, Addison Wesley Longman, Harlow (1999).
[32] *Chem. Rev*., **105**(6) (2005).
[33] D.R. Stranks. *Pure Appl. Chem*., **38**, 303 (1974).
[34] R. van Eldik, C.D. Hubbard. In *Application of High Pressure in Inorganic and Bioinorganic Chemistry, in Chemistry under Extreme Conditions*, R.R. Manaa (Ed.), Chapter 4, Elsevier, Amsterdam (2005).
[35] R. van Eldik, C.D. Hubbard. The interpretation and mechanistic significance of activation volumes for organometallic reactions, in *Adv. Phys. Org. Chem*., J. Richard, Ed., Vol. 41, 1 (2006).
[36] A. Drljaca, C.D. Hubbard, R. van Eldik, T. Asano, M.V. Basilevsky, W.J. le Noble. *Chem. Rev*., **98**, 2167 (1998).
[37] R. van Eldik, C. Dücker-Benfer, F. Thaler. *Adv. Inorg. Chem*., **49**, 1 (2000).
[38] R. van Eldik, C.D. Hubbard. In *Effect of Pressure on Inorganic Reactions: Introduction and Mechanistic Applications, in High Pressure Chemistry: Synthetic, Mechanistic and Supercritical Applications*, R. van Eldik, F.-G. Klärner (Eds), Chapter 1, Wiley-VCH, Weinheim (2002).
[39] D.T. Richens. *The Chemistry of Aquaions*, John Wiley, Chichester (1997).
[40] *Adv. Inorg. Chem*., **54** (2003).
[41] P.W. Atkins. *Physical Chemistry*, 4th Edn, Freeman, New York (1990).
[42] D.A. Palmer, H. Kelm. *Coord. Chem. Rev*., **36**, 89 (1981).
[43] A.E. Merbach. *Pure Appl. Chem*., **54**, 1479 (1982).
[44] M.J. Blandamer, J. Burgess. *Pure Appl. Chem*., **55**, 55 (1983).
[45] P. Moore. *Pure Appl. Chem*., **57**, 347 (1985).
[46] R. van Eldik (Ed.). *Inorganic High Pressure Chemistry*, *Kinetics and Mechanism*, Elsevier, Amsterdam (1986).
[47] M. Kotowski, R. van Eldik. *Coord. Chem. Rev*., **93**, 19 (1989).
[48] C.D. Hubbard, R. van Eldik. *Instrumentation Sci. Tech*., **23**, 1 (1995).
[49] S.F. Lincoln, A.E. Merbach. *Adv. Inorg. Chem*., **42**, 11 (1995).
[50] R. van Eldik, C.D. Hubbard. In *Effect of Pressure on Inorganic Reactions, in Chemistry under Extreme or Non-Classical Conditions*, R. van Eldik, C.D. Hubbard (Eds), Chapter 2, Spektrum-Wiley, Heidelberg-New York (1997).
[51] W.B. Holzapfel, N.S. Isaacs (Eds). *High Pressure Techniques in Chemistry and Physics – A Practical Approach*, Oxford University Press, Oxford (1997).
[52] R. van Eldik, C.D. Hubbard. *S. Afr. J. Chem*., **52**, 139 (2000).
[53] L. Helm, A.E. Merbach. *J. Chem. Soc., Dalton Trans*., **633** (2002).
[54] K. Ishihara, S. Funahashi, M. Tanaka. *Rev. Sci. Instrum*., **53**, 1231 (1982).
[55] K. Ishihara, Y. Kondo, M. Koizumi. *Rev. Sci. Instrum*., **70**, 244 (1999).
[56] R. van Eldik, D.A. Palmer, R. Schmidt, H. Kelm. *Inorg. Chim. Acta*, **50**, 131 (1981).
[57] R. van Eldik, W. Gaede, S. Wieland, J. Kraft, M. Spitzer, D.A. Palmer. *Rev. Sci. Instrum*., **64**, 1355 (1993).
[58] A. Zahl, P. Igel, M. Weller, D. Koshtariya, M.S.A. Hamza, R. van Eldik. *Rev. Sci. Instrum*., **74**, 3758 (2003).
[59] A. Zahl, P. Igel, M. Weller, R. van Eldik. *Rev. Sci. Instrum*., **75**, 3152 (2004).
[60] R. van Eldik, P.C. Ford. *Adv. Photochem*., **24**, 61 (1998).
[61] T.W. Swaddle. *Chem. Rev*., **105**, 2573 (2005).
[62] R. van Eldik, D. Meyerstein. *Acc. Chem. Res*. **33**, 207 (2000); A. Masarwa, D. Meyerstein. *Adv. Inorg. Chem*. **55**, 271 (2004).
[63] C.A. Eckert. *Annu Rev. Phys. Chem*., **23**, 239 (1972).
[64] G. Jenner. *Angew. Chem. Int. Ed*., **14**, 137 (1975).
[65] G. Jenner. *J. Phys. Org. Chem*., **15**, 1 (2002).
[66] T. Asano, W.J. le Noble. *Chem. Rev*., **78**, 407 (1978).
[67] R. van Eldik, T. Asano, W.J. le Noble. *Chem. Rev*., **89**, 549 (1989).
[68] L. Helm, A.E. Merbach. In *High Pressure Chemistry. Synthetic, Mechanistic and Supercritical Applications*, R. van Eldik, F.-G. Klärner (Eds), Chapter 4, Wiley-VCH, Weinheim (2002).
[69] F. Dunand, L. Helm, A.E. Merbach. *Adv. Inorg. Chem*., **54**, 1 (2003).
[70] References loc cit in references (68) and (69).
[71] T. Mizuta, J. Wang, K. Miyoshi. *Inorg. Chim. Acta*, **175**, 221 (1990).
[72] X. Solans, M. Font-Altaba, J. Oricain. *Acta Crystallogr. Sect. C*, 635 (1984).
[73] T. Schneppensieper, S. Seibig, A. Zahl, P. Tregloan, R. van Eldik. *Inorg. Chem*., **40**, 3670 (2001).
[74] T.W. Swaddle, A.E. Merbach. *Inorg. Chem*., **20**, 4212 (1981).
[75] M. Grant, R.B. Jordan. *Inorg. Chem*., **20**, 55 (1981).

[76] M. Mizuno, S. Funahashi, N. Nakasuka, M. Tanaka. *Inorg. Chem.*, **30**, 1550 (1991).
[77] P. Caravan, E. Töth, A. Rockenbauer, A.E. Merbach. *J. Am. Chem. Soc.*, **121**, 10403 (1999).
[78] E. Töth, L. Burai, A.E. Merbach. *Coord. Chem. Rev.*, **216–217**, 363 (2001).
[79] G. Moreau, L. Helm, J. Purans, A.E. Merbach. *J. Phys. Chem. A*, **106**, 3034 (2002).
[80] P. Caravan, J.J. Ellison, T.J. McMurry, R.B. Lauffer. *Chem. Rev.*, **99**, 2293 (1999).
[81] *The Chemistry of Contrast Agents in Medical Magnetic Resonance Imaging*, 1st Edn, A.E. Merbach, E. Töth (Eds). John Wiley and Sons, Chichester (2001).
[82] E. Töth, L. Helm, A.E. Merbach. In *Magnetic Contrast Agents*, W. Krause (Ed.), Springer, Heidelberg (2001).
[83] M.K. Thompson, M. Botta, G. Nicholle, L. Helm, S. Aime, A.E. Merbach, K.N. Raymond. *J. Am. Chem. Soc.*, **125**, 14274 (2003).
[84] L. Burai, E. Töth, G. Moreau, A. Sour, R. Scopelliti, A.E. Merbach. *Chem. Eur. J.*, **9**, 1394 (2003).
[85] U. Prinz, U. Koelle, S. Ulrich, A.E. Merbach, O. Maas, K. Hegetschweiler. *Inorg. Chem.*, **43**, 2387 (2004).
[86] S. Laus, R. Ruloff, E. Töth, A.E. Merbach. *Chem. Eur. J.*, **9**, 3555 (2003).
[87] G. Moreau, L. Burai, L. Helm, J. Purans, A.E. Merbach. *J. Phys. Chem. A*, **107**, 758 (2003).
[88] G.M. Nicholle, F. Yerly, D. Imbert, U. Böttger, J.-C. Bünzli, A.E. Merbach. *Chem. Eur. J.*, **9**, 5453 (2003).
[89] R. Ruloff, G. van Koten, A.E. Merbach. *Chem. Commun.*, 842 (2004).
[90] P.S. Salmon, G.W. Neilson, J.E. Enderby. *J. Phys. C Solid State Phys.*, **21**, 1335 (1988).
[91] D.H. Powell, L. Helm, A.E. Merbach. *J. Chem. Phys.*, **95**, 9258 (1991).
[92] D.H. Powell, P. Furrer, P. Pittet, A.E. Merbach. *J. Phys. Chem.*, **99**, 16622 (1995).
[93] A. Pasquarello, I. Petri, P.S. Salmon, O. Parisel, R. Car, E. Toth, D.H. Powell, H.E. Fischer, L. Helm, A.E. Merbach. *Science*, **291**, 856 (2001).
[94] I. Persson, P. Persson, M. Sandström, A.-S. Ullström. *J. Chem. Soc. Dalton Trans.*, 1256 (2002).
[95] References 9, 11, 16–22 in Reference 92.
[96] M. Benfatto, P. D'Angelo, S. Della Longa, N.V. Pavel. *Phys. Rev. B*, **65**, 174201 (2002).
[97] J.H. Coates, P.R. Collins, S.F Lincoln. *J. Chem. Soc., Faraday Trans.* **75**, 1236 (1979); J.H. Coates, P.R. Collins, S.F. Lincoln. *Aust. J. Chem.* **33**, 1381 (1980); S.F. Lincoln, C.D. Hubbard. *J. Chem. Soc., Dalton Trans.* 2513 (1974), and references loc cit.
[98] D.H. Powell, A.E. Merbach, I. Fabian, S. Schindler, R. van Eldik. *Inorg. Chem.*, **33**, 4468 (1994).
[99] F. Thaler, C.D. Hubbard, F.W. Heinemann, R. van Eldik, S. Schindler, I. Fabian, A.M. Dittler-Klingemann, F.E. Hahn, C. Orvig. *Inorg. Chem.*, **37**, 4022 (1998).
[100] A. Neubrand, F. Thaler, M. Körner, A. Zahl, C.D. Hubbard, R. van Eldik. *J. Chem. Soc., Dalton Trans.*, 957 (2002).
[101] A.M. Dittler-Klingemann, C. Orvig, F.E. Hahn, F. Thaler, C.D. Hubbard, R. van Eldik, S. Schindler, I. Fabian. *Inorg. Chem.*, **35**, 7798 (1996).
[102] G.U. Priimov, P. Moore L. Helm, A.E. Merbach. *Inorg. React. Mech.*, **3**, 1 (2001).
[103] I. Ivanovic-Burmazovic, M.S.A. Hamza, R. van Eldik. *Inorg. Chem.*, **45**, 1575 (2006).
[104] I. Ivanovic-Burmazovic, M.S.A. Hamza, R. van Eldik. *Inorg. Chem. Commun.*, **5**, 937 (2002).
[105] I. Ivanovic-Burmazovic, M.S.A. Hamza, R. van Eldik. *Inorg. Chem.*, **41**, 5150 (2002).
[106] I. Ivanovoc-Burmazovic, K. Andjelkovic. *Adv. Inorg. Chem.*, **55**, 315 (2004).
[107] R.H. Holyer, C.D. Hubbard, S.F.A. Kettle, R.G. Wilkins. *Inorg. Chem.*, **4**, 929 (1965).
[108] M. Eigen, K. Tamm. *Z. Elektrochem.*, **66**, 107 (1962).
[109] R.G. Wilkins. *Inorg. Chem.*, **3**, 520 (1964).
[110] D. Rablen, G. Gordon. *Inorg. Chem.*, **8**, 395 (1969).
[111] G.R. Cayley, D.W. Margerum. *J. Chem. Soc., Chem. Commun.*, 102 (1994).
[112] G.U. Priimov, P. Moore. *Inorg. React. Mech.*, **5**, 21 (2003).
[113] P.R. Mitchell, H. Sigel. *J. Am. Chem. Soc.*, **100**, 1564 (1978).
[114] R.E. Shepherd, Y. Chen, S. Zang, F.T. Lin, A. Kortes. in *Electron Transfer Reactions*, S. Isied (Ed.), Advances in Chemistry Series, Vol. 253, pp. 367–398, American Chemical Society (1997).
[115] D. Chatterjee, M.S.A. Hamza, M.M. Shoukry, A. Mitra, S. Deshmukh, R. van Eldik. *Dalton Trans.*, 203 (2003).
[116] M.M. Shoukry, M.R. Shehata, M.S.A. Hamza, R. van Eldik. *Dalton Trans.*, 3921 (2005).
[117] R.A. Alderden, M.D. Hall, T.W. Hambley. *J. Chem. Educ.*, **83**, 728 (2006).
[118] N. Summa, W. Schiessl, R. Puchta, N. van Eikema Hommes, R. van Eldik. *Inorg. Chem.*, **45**, 2948 (2006).
[119] A. Hofmann, D. Jaganyi, O.Q. Munro, G. Liehr, R. van Eldik. *Inorg. Chem.*, **42**, 1688 (2003).
[120] Z.D. Bugarcic, G. Liehr, R. van Eldik. *J. Chem. Soc., Dalton Trans.*, 2825 (2002).
[121] Z.D. Bugarcic, G. Liehr, R. van Eldik. *J. Chem. Soc., Dalton Trans.*, 951 (2002).
[122] Z.D. Bugarcic, F.W. Heinemann, R. van Eldik. *Dalton Trans.*, 279 (2004).
[123] Z.D. Bugarcic, T. Soldatovic, R. Jelic, B. Alguero, A. Grandas. *Dalton Trans.*, 3869 (2004).
[124] T. Soldatovic, Z.D. Bugarcic. *J. Inorg. Biochem.*, **99**, 1472 (2005).
[125] C.F. Weber, R. van Eldik. *Eur. J. Inorg. Chem.*, 4755 (2005).

[126] D. Jaganyi, F. Tiba, O.Q. Munro, B. Petrovic, Z. Bugarcic. *Dalton Trans*., 2943 (2006).
[127] Reference 31, page 84.
[128] A.A. El-Sherif, M.M. Shoukry, R. van Eldik. *J. Chem. Soc., Dalton Trans*., 1425 (2003).
[129] A.A. Al-Najjar, M.M. Mohamed, M.M. Shoukry. *J. Coord. Chem*., **59**, 193 (2006).
[130] S.K. Mukhopadhyay, A.K. Ghosh. *Inorg. React. Mech*., **5**, 255 (2005).
[131] S.K. Mukhopadhyay, A.K. Ghosh. *Inorg. React. Mech*., **6**, 9 (2006).
[132] M.P. Lowe, D. Parker, O. Reany, S. Aime, M. Botta, G. Castellano, E. Gianolio, R. Pagliarin. *J. Am. Chem. Soc*., **123**, 7001 (2001).
[133] E. Szilágyi, E. Brücher. *J. Chem. Soc., Dalton Trans*., 2239 (2000).
[134] E. Szilágyi, E. Töth, Z. Kovács, J. Platzek, B. Radüchel, E. Brücher. *Inorg. Chim. Acta*, **298**, 226 (2000).
[135] M. Birus, M. Gabricievic, O. Cronja, B. Klaic, R. van Eldik, A. Zahl. *Inorg. Chem*., **38**, 4064 (1999).
[136] M. Birus, R. van Eldik, M. Gabricevic, A. Zahl. *Eur. J. Inorg. Chem*., 819 (2002).
[137] L. Valzelli, S. Garattini. In *Principles of Psychopharmacology*, W.G. Clark (Ed.), p. 255, Academic Press, New York (1970).
[138] M. Sainsbury. In *Comprehensive Heterocyclic Chemistry*, A.R. Katritsky, C.W. Rees (Eds), Vol. 3, p. 995, Pergamon Press, Oxford (1984).
[139] E. Pelizzetti, E. Mentasti. *Inorg. Chem*., **18**, 583 (1979).
[140] R. van Eldik, J. Wisniewska. *Inorg. Chem*., **41**, 3802 (2002).
[141] J. Wisniewska, R. van Eldik. *Inorg. React. Mech*., **6**, 1 (2006).
[142] J.I. Sachinidis, R.D. Shalders, P. A Tregloan. *Inorg. Chem*., **35**, 2497 (1996).
[143] R.A. Marcus. *J. Phys. Chem*., **72**, 891 (1968).
[144] N.S. Hush. *Coord. Chem. Rev*., **64**, 135 (1985).
[145] T.W. Swaddle. *Inorg. Chem*., **29**, 5017 (1990).
[146] M.R. Grace, H. Takagi, T.W. Swaddle. *Inorg. Chem*., **33**, 1915 (1994).
[147] W.H. Jolley, D.R. Stranks, T.W. Swaddle. *Inorg. Chem*., **29**, 1948 (1990).
[148] M. Körner, R. van Eldik. *Eur. J. Inorg. Chem*., 1805 (1999).
[149] J. Macyk, R. van Eldik. *J. Chem. Soc., Dalton Trans*., 2288 (2001).
[150] I. Krack, R. van Eldik. *Inorg. Chem*., **25**, 1743 (1986).
[151] J. Sun, J.F. Wishart, R. van Eldik, R.D. Shalders, T.W. Swaddle. *J. Am. Chem. Soc*., **117**, 2600 (1995).
[152] M. Körner, P.A. Tregloan, R. van Eldik. *Dalton Trans*., 2710 (2003).
[153] Y. Fu, T.W. Swaddle. *Inorg. Chem*., **38**, 876 (1999).
[154] J.I. Sachinidis, R.D. Shalders, T.W. Swaddle. *Inorg. Chem*., **33**, 6180 (1994).
[155] T.W. Swaddle, P.A. Tregloan. *Coord. Chem. Rev*., **187**, 255 (1999).
[156] T.W. Swaddle. *Inorg. Chem*., **22**, 2665 (1983).
[157] B. Bänsch, M. Meier, P. Martinez, R. van Eldik, C. Su, J. Sun, S.S. Isied, J.F. Wishart. *Inorg. Chem*., **33**, 4744 (1994).
[158] M. Meier, J. Sun, J.F. Wishart, R. van Eldik. *Inorg. Chem*., **35**, 1564 (1996).
[159] D.S. Bredt, P.M. Hwang, C.E. Glatt, C. Lowenstein, R.R. Reed, S.H. Snyder. *Nature*, **351**, 714 (1991).
[160] A.R. Butler, D.L.H. Williams. *Chem. Soc. Rev*., **22**, 233 (1993).
[161] R.J.P. Williams. *Chem. Soc. Rev*., **25**, 77 (1996).
[162] Q.H. Gibson, F.J.W. Roughton. *J. Physiol*., **136**, 507 (1957).
[163] B.M. Hoffman, Q.H. Gibson. *Proc. Natl. Acad. Sci. U.S.A*., **75**, 21 (1978).
[164] M.L. Cairson, R. Regen, E. Elber, H. Li, G.N. Phillips, J.L. Olson, Q.H. Gibson. *Biochemistry*, **33**, 10597 (1994).
[165] M. Hoshino, L.E. Laverman, P.C. Ford. *Coord. Chem. Rev*., **187**, 75 (1999).
[166] L.E. Laverman, A. Wanat, J. Oszajca, G. Stochel, P.C. Ford, R. van Eldik. *J. Am. Chem. Soc*., **123**, 285 (2001).
[167] A. Wanat, J. Gdula-Argasinska, D. Rutowska-Zbik, M. Witko, G. Stochel, R. van Eldik. *J. Biol. Inorg. Chem*., **7**, 165 (2002).
[168] L.E. Laverman, M. Hoshino, P.C. Ford. *J. Am. Chem. Soc*., **119**, 12663 (1997).
[169] L.E. Laverman, P.C. Ford. *Chem. Commun*., 1843 (1999).
[170] L. Miller, A.J. Pedraza, M.R. Chance. *Biochemistry*, **36**, 12199 (1997).
[171] A.M. Rich, R.S. Armstrong, P.J. Ellis, P.A. Lay. *J. Am. Chem. Soc*., **120**, 10827 (1998).
[172] M. Feelish, J.S. Stamler (Eds). *Methods in Nitric Oxide Research*, John Wiley and Sons, Chichester (1996), and references *loc. cit*.
[173] A.C. Anusiem, J.G. Beetlestone, D.H. Irvine. *J. Chem. Soc. A*, 357 (1966); *ibid* 960, (1968); *ibid* 1346 (1968) *ibid* 960, (1968); *ibid* 1346.
[174] J. Mintorovitch, J.D. Satterlee. *Biochemistry*, **27**, 80 (1968).
[175] A. Brancaccio, F. Cutuzzola, C.T. Allocatelli, M. Brunori, S.J. Smerdon, A.J. Wilkinson, Y. Dou, D. Keenan, M. Ikeda-Saito, R.E. Brantley, J.S. Olson. *J. Biol. Chem*., **269**, 13843 (1994).
[176] Y. Dou, J.S. Olson, A.J. Wilkinson, M. Ikeda-Saito. *Biochemistry*, **35**, 7107 (1996).
[177] Q.H. Gibson, L.J. Parkhurst, G. Geraci. *J. Biol. Chem*., **244**, 4668 (1969).
[178] J.-E. Jee, S. Eigler, F. Hampel, N. Jux, M. Wolak, A. Zahl, G. Stochel, R. van Eldik. *Inorg. Chem*., **44**, 7717 (2005) and references *loc cit*.

[179] A. Cusanelli, U. Frey, D.T. Richens, A.E. Merbach. *J. Am. Chem. Soc.*, **118**, 5265 (1996).
[180] A. Franke, G. Stochel, C. Jung, R. van Eldik. *J. Am. Chem. Soc.*, **126**, 4181 (2004).
[181] J.-E. Jee, M. Wolak, D. Balbinot, N. Jux, A. Zahl, R. van Eldik. *Inorg. Chem.*, **45**, 1326 (2006).
[182] T. Schneppensieper, S. Winkler, A. Czap, R. van Eldik, M. Heus, P. Nieuwenhuizen, C. Wreesmann, W. Abma. *Eur. J. Inorg. Chem.*, 491 (2001).
[183] T. Schneppensieper, A. Wanat, G. Stochel, S. Golstein, D. Meyerstein, R. van Eldik. *Eur. J. Inorg. Chem.*, **2317** (2001).
[184] A. Theodoridis, R. van Eldik. *J. Mol. Catal. A: Chem.*, **224**, 197 (2005).
[185] A. Czap, F.W. Heinemann, R. van Eldik. *Inorg. Chem.*, **43**, 7832 (2004).
[186] A. Franke, G. Stochel, N. Suzuki, T. Higuchi, K. Okuzono, R. van Eldik. *J. Am. Chem. Soc.*, **127**, 5360 (2005).
[187] M. Wolak, R. van Eldik. *J. Am. Chem. Soc.*, **127**, 13312 (2005).
[188] F. Roncaroli, R. van Eldik. *J. Am. Chem. Soc.*, **128**, 8042 (2006).
[189] C.-H. Kwak, J.-E. Jee, M. Pyo, J. Kim, R. van Eldik. *Inorg. Chim. Acta*, **357**, 2643 (2004).
[190] D.M. Heinekey, A. Lledos, J.M. Lluch. *Chem. Soc. Rev.*, **33**, 175 (2004).
[191] S.G. Yan, B.S. Brunschwig, C. Creutz, E. Fujita, N. Sutin. *J. Am. Chem. Soc.*, **120**, 10553 (1998).
[192] E. Fujita, B.S. Brunschwig, C. Creutz, J.T. Muckerman, N. Sutin, D. Szalda, R. van Eldik. *Inorg. Chem.*, **45**, 1595 (2006).
[193] R. Schmidt, M. Geis, H. Kelm. *Z. Phys. Chem.*, **92**, 223 (1974).
[194] E. Fujita, R. van Eldik. *Inorg. Chem.*, **37**, 360 (1998).
[195] E. Fujita, J.F. Wishart, R. van Eldik. *Inorg. Chem.*, **41**, 1579 (2002).
[196] J.D. Artis, S. Vinogradov, B. Zak. *Clin. Biochem.*, **14**, 311 (1981).
[197] T. Higgins. *Clin. Chem.*, **27**, 1619 (1981).
[198] L.H. Stookey. *Analyt. Chem.*, **42**, 779 (1970).
[199] C.R. Gibbs. *Analyt. Chem.*, **48**, 1197 (1976).
[200] J. Burgess, D.L. Duke, C.D. Hubbard. *Trans. Met. Chem.*, **12**, 460 (1987).
[201] R.D. Gillard. *Inorg. Chim. Acta*, **11**, L21 (1974).
[202] R.D. Gillard. *Coord. Chem. Rev.*, **16**, 67 (1975).
[203] J. Burgess, C.D. Hubbard, P.H. Miyares, T.L. Cole, T.P. Dasgupta, S. Leebert. *Trans. Met. Chem.*, **30**, 957 (2005).
[204] D.W. Margerum, L.P. Morgenthaler. *J. Am. Chem. Soc.*, **84**, 706 (1962).
[205] R. Romeo, L. Fenech, L.M. Scolaro, A. Albinati, A. Macchioni, C. Zuccaccia. *Inorg. Chem.*, **40**, 3293 (2001).
[206] R. Romeo, L. Fenech, S. Carnabuchi, M.R. Plutino, A. Romeo. *Inorg. Chem.*, **41**, 2839 (2002).
[207] R. Romeo, S. Carnabuchi, M.R. Plutino, A. Romeo, S. Rizzato, A. Albinati. *Inorg. Chem.*, **44**, 1248 (2005).
[208] R. Romeo, S. Carnabuchi, L. Fenech, M.R. Plutino, A. Albinati. *Angew. Chem.*, **118**, 4606 (2006).
[209] H. Erras-Hanauer, T. Clark, R. van Eldik. *Coord. Chem. Rev.*, **238–239**, 233 (2003).
[210] C. Selcuki, R. van Eldik, T. Clark. *Inorg. Chem.*, **43**, 2828 (2004).
[211] References cited in reference 210.
[212] P.-A. Pittet, G. Elbaze, L. Helm, A.E. Merbach. *Inorg. Chem.*, **29**, 1936 (1990).
[213] R. Puchta, N. van Eikema Hommes, R. van Eldik. *Helv. Chim. Acta*, **88**, 911 (2005).
[214] D. Spanberg, R. Roy, J.T. Hynes, K. Hermansson. *J. Phys. Chem. B*, **107**, 4470 (2003).
[215] R. Puchta, M. Galle, N. van Eikema Hommes, E. Pasgreta, R. van Eldik. *Inorg. Chem.*, **43**, 8227 (2004).